Simultaneous Optimal Design of Multi-Stage Organic Rankine Cycles and Working Fluid Mixtures for Low-Temperature Heat Sources

David M. Thierry[1], Antonio Flores-Tlacuahuac*[1] and Ignacio E. Grossmann[2]

[1]Departamento de Ingeniería y Ciencias Químicas, Universidad Iberoamericana, Prolongación Paseo de la Reforma 880, México D.F., 01219, México.

[2]Department of Chemical Engineering, Carnegie-Mellon University, 5000 Forbes Av., Pittsburgh 15213, PA

October 26, 2015

*Author to whom correspondence should be addressed. E-mail: antonio.flores@ibero.mx, phone/fax:+52(55)59504074, http://200.13.98.241/∼antonio

Abstract

Energy recovery is a process strategy seeking to improve process efficiency through the capture, recycle and deployment of normally neglected low energy content sources or streams. By proper optimal process design, such low-temperature energy sources can be a feasible and economical manner of approaching the energy recovery issue. In particular, when Rankine cycles with mixtures as working fluids are used, the amount of energy recovery can be improved. The formulation and systematic solution of this problem has shown better results when all the variables of the Rankine cycle and the compositions of the working fluid are considered simultaneously. Another interesting approach is the implementation of multiple cycles coupled together. In this work we propose a nonlinear optimization formulation of two general multistage approaches for the Rankine cycle with mixtures: the cascade and series configurations. As main decision variables, we have considered the heat source conditions and the mixture components. Then, the resulting optimization problem is solved in a deterministic approach as a nonlinear program. The results shown that for some cases the multistage configurations are useful but limited in terms of cost in comparison to the single stage cycle.

1 Introduction

The generation of energy with low-environmental cost technologies is an important matter that has been continuously assessed over the years. One particular appealing idea is conversion of low-temperature heat to power by means of an Organic Rankine Cycle (ORC) [1, 2]. The performance of the ORC can be improved by several strategies, like modifications of the cycle configuration, pure and mixture working fluids selection and design. Linke et al. [3] performed an in depth review of the state of the art systematic methods for the ORC design.

Recent approaches on the selection and design of the working fluid, either pure or mixture include the following works. Mavrou et al. [4] investigated the selection of working fluid mixtures through sensitivity analysis; their framework enabled them to identify the operating parameters whose variation impacted the ORC performance the most, and the mixture which has the best performance under variable conditions. Braimakis et al. [5] investigated several pure fluids and binary mixtures with both sub-critical and supercritical operations. They found that the supercritical ORC with low critical temperature fluids and moderate to high heat source temperatures displays an increase of exergetic efficiency. Lampe et al. [6] created a framework for the simultaneous selection of the working fluid and process optimization through a continuous molecular targeting approach. They were able to identify the best performing fluids from a large database. Lecompte et al. [7] presented an overview of the ORC architectures.

A relevant work on the simultaneous mixture and operating conditions selection by means of nonlinear optimization was previously presented [8]. In this work a nonlinear model was developed and solved for a set of case studies. It was found that optimal mixtures only require a few components; forcing additional species into the mixture does not improve the efficiency of the cycle.

As part of the cycle configuration approaches, the multistage concept has been devel-

oped by various authors with a number of configurations. The basic idea is to consider several pieces of equipment, so more power is generated or a less costly scheme is obtained. In this regard, Kosmadakis et al. [9] carried out an economic assessment of a two-stage Solar Organic Rankine Cycle that drives an desalinization unit. The evaluated cycle in this paper is in a cascade configuration, and showed a better efficiency and lower specific cost than a single-stage. Morisaki et al. [10] introduced a formula for the calculation of the maximum power of a multistage heat engine (which is the basic idea of the series configuration in this work). They found that the multi-stage configuration doubled the power in comparison to the single-stage, although the efficiency is constant regardless the number of stages. Yun et al. [11] evaluated an experimental ORC with multiple expanders that works in parallel. They found the multiple expander design is better than the basic-ORC when they are subject to large variations in the amounts of waste heat produced. Li et al. [12] evaluated the performance of two configurations of ORCs where the heat source is segmented into two temperature ranges. They found that the series configuration has better performance than the parallel cycle. Stijepovic et al. [13] developed a mathematical model based on the exergy composite curves for the analysis of ORCs with a multi-pressure configuration. Then, they implemented an optimization strategy that determined the number of pressure loops and operating parameters.

The potential of simultaneous multiple Rankine cycles is generally recognized, although there are many different configurations, it is necessary to develop a generic scheme of multistage ORCs and to draw a conclusion on the improvements.

Additionally, the design of the working fluid mixtures for this kind of configurations has not been addressed. It is possible to implement an individual mixture for each stage, and have stages absorbing heat in various ways. With this, it is also possible to compare the cost implications of these configurations and draw a conclusion on their potential.

Therefore, in this work we propose the extension of ORCs with mixtures to multistage configurations, all developed with an equation oriented approach, meaning that every

aspect from thermodynamics to cost constraints are included and solved simultaneously in a nonlinear optimization model. To our best knowledge, such a problem has not been considered in the open research literature.

2 Problem Definition

The appropriate selection of the operating conditions and mixture composition is a way of increasing the efficiency of the power generation of the Rankine Cycle (RC) with low-temperature heat sources. But even in the most efficient RC, heat rejection is considerable and unavoidable. Because we are still far from the upper limit imposed by the thermodynamics, it is reasonable to assume that by absorbing more heat by means of a more complex scheme, the efficiency of the cycle would be better than that achieved by the simple RC.

A natural way of trying to absorb more heat than in a single RC would be using a second cycle at the same time. How the second RC should be coupled with the heat source is a more complicated issue if we consider that there is no unique way of doing this. A single RC takes heat from the heat source (HS) in the vaporizer (Figure 1). We could partition the HS stream and send the resulting streams to an individual RC (in this case two HS streams two RCs). If we recognize that the HS heat content could also be partitioned, then every part of the heat could be used in a RC. This is the idea of the series-connected RC (Figure 2). The main difference between these two processes is that the first one is a *physical* split of the HS stream, while the second is an *energy* split.

If we try to find the optimal operating conditions from the above stated configurations, we would find that only the second one (i.e. the Series RC) matters, because if we set-up a molar basis model the solution of the first one would be two identical cycles (or the single cycle solution). Also, the second problem would be the determination of the optimal operating conditions and the composition of the working fluid mixtures for each

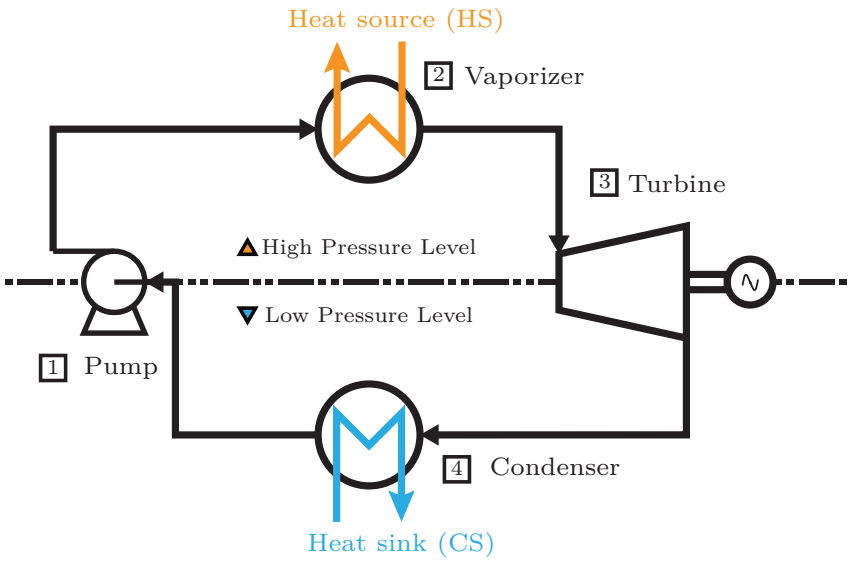

Figure 1: The Rankine Cycle

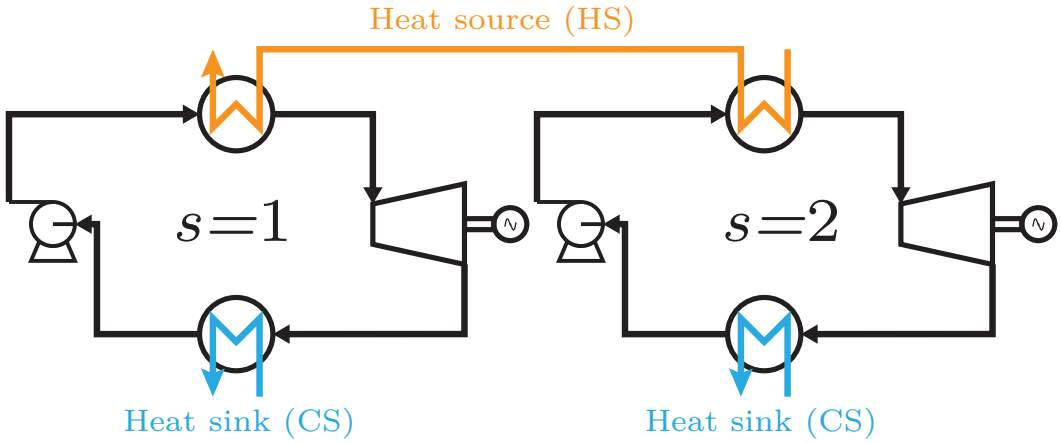

Figure 2: Two-stage Series flow diagram

cycle simultaneously.

Other possible configuration revolves around the fact that every individual RC has to reject heat. A second cycle can take the rejected heat from the first cycle and then to generate power from it. This succession ends in the rejection of heat to the sink by the second cycle and is the basic idea of the Cascade configuration is shown in Figure 3.

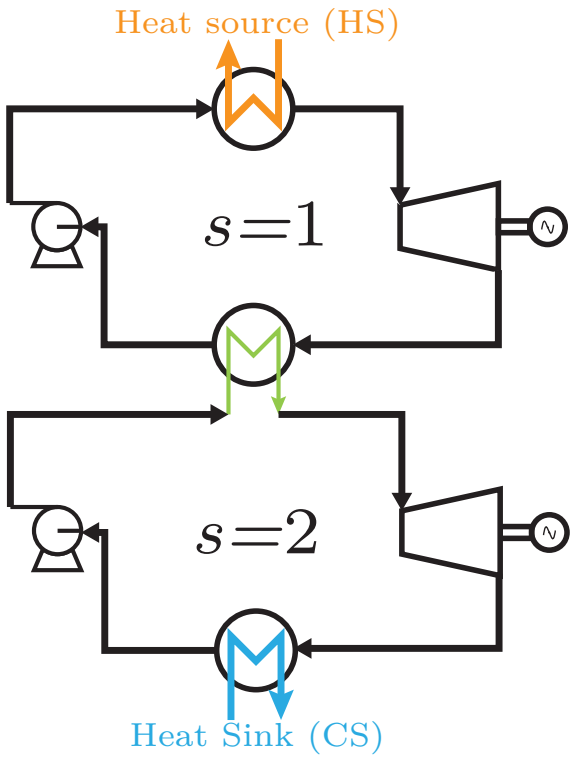

Figure 3: Two-stage Cascade flow diagram

Every consecutive cycle in the Cascade configuration would have to absorb a smaller amount of heat, and possibly minimize the heat rejection. The two configurations of multiple RCs can be further generalized as shown by the Figures 4 and 5, where a large number of cycles can be implemented.

Naturally we can expect some impact on the efficiency of the overall cycle. But it is also important to consider the economic implications in terms of what these configurations do to the price that we have to pay for the electricity produced. This is why the sizing of the equipment becomes a necessity. With all this information comprised into a model,

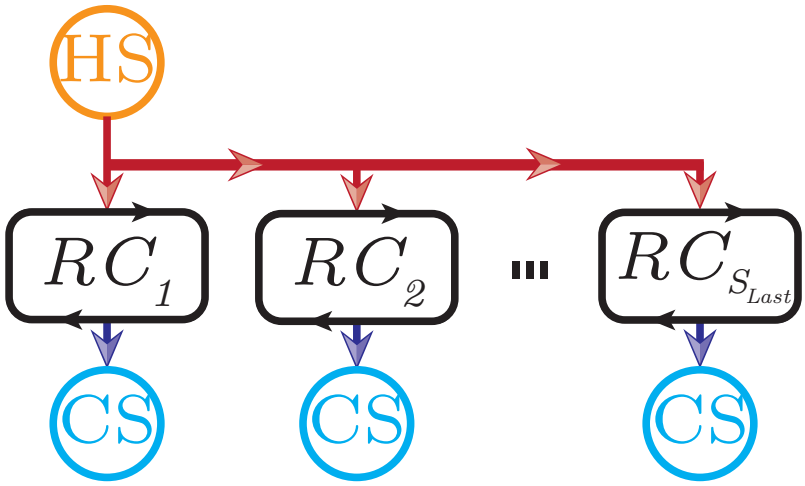

Figure 4: The series configuration, a heat flow from Source (HS) to Rankine cycles (RC) and to the Heat Sinks (CS).

we can make decisions on the mixtures that are used as working fluids, and the operating conditions at which the cycle is carried out.

Assuming that several sources of low-temperature heat are available, and that maximum heat recovery (trough power generation) is desired, then, there are two key elements that we can exploit to achieve this goal: (a) a set of multistage series/cascade Rankine cycles with variable pressures, temperatures, flows, etc.; and (b) a working fluid that is mixture of a set of predefined components suitable for the low-temperature application with variable composition.

The problem to be addressed in this work can be stated as follows: "For a given low-temperature heat source the problem consists in simultaneously obtaining the optimal mixture composition of the working fluid from some predefined components, and the optimal operating conditions of a set of series or cascade coupled Rankine cycles such that to maximum energy recovery or minimum electricity cost are achieved".

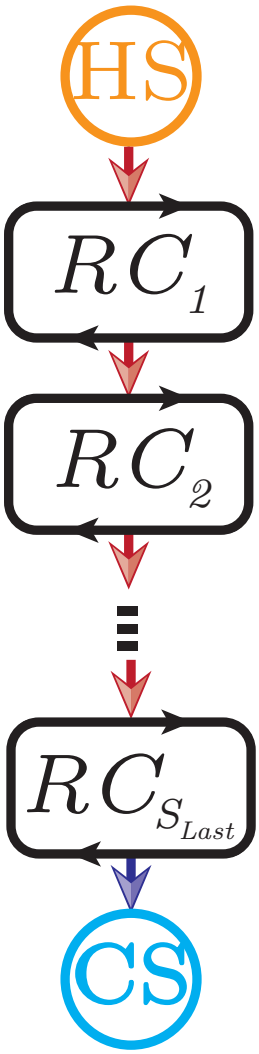

Figure 5: The cascade scheme. Heat flow from Heat Source (HS) through Rankine cycles (RC) to the Heat Sink (CS)

3 Optimization Formulation

3.1 Sets

The sets required for the algebraic formulation of the problem are defined as follows:

- The Available chemical species $i, j \in I$
- The stage $s \in S_{TG} = \{1, 2, .., S_L\}$; if the cycle is single stage then $S_{TG} = \{1\}$.
- The UNIFAC functional group $k, m, n \in M$ related to the activity coefficients.
- The phase $f \in F =$ { Liquid(L),Vapor(V) }, for calculations that are for a particular phase.
- The equilibrium or two phase point $\pi \in \Pi =$ {Bubl,1,2,3,..,Dew} (1,2,3, are internal points between bubble and dew point).
- The pressure level $p \in L =$ { High,Low }, which relates to its location in the cycle.
- The subcool $\underline{o} \in \underline{O}$={Sub,SubS} and superheat (nonisentropic,isentropic) $\overline{o} \in \overline{O}$ ={Over,OverS} ; $\overline{O} \cup \underline{O} = O$. Which imply variables that are not at equilibrium and are exclusive for single phase.

Moreover, it should be noted that there are two main groups of variables, the off-superheat/subcool and the on-superheat/subcool (denoted with the index o).

The optimization algebraic models are summarized in Figure 7. The equations are distributed in four main groups: (1) the equation of state group $\overline{\boldsymbol{Z}}_s$ which contains information related to the compressibility factors; (2) the activity coefficients $\overline{\boldsymbol{G}}_s$ which contain the core of the UNIFAC method of activity coefficients; (3) the equilibrium and property set $\overline{\boldsymbol{B}}_d$ which contains the enthalpy, entropy, fugacity and equilibrium relationships; and (4) the $\overline{\boldsymbol{\varphi}}_s$ constraints that are comprised of the isentropic, nonisentropic, heat and work

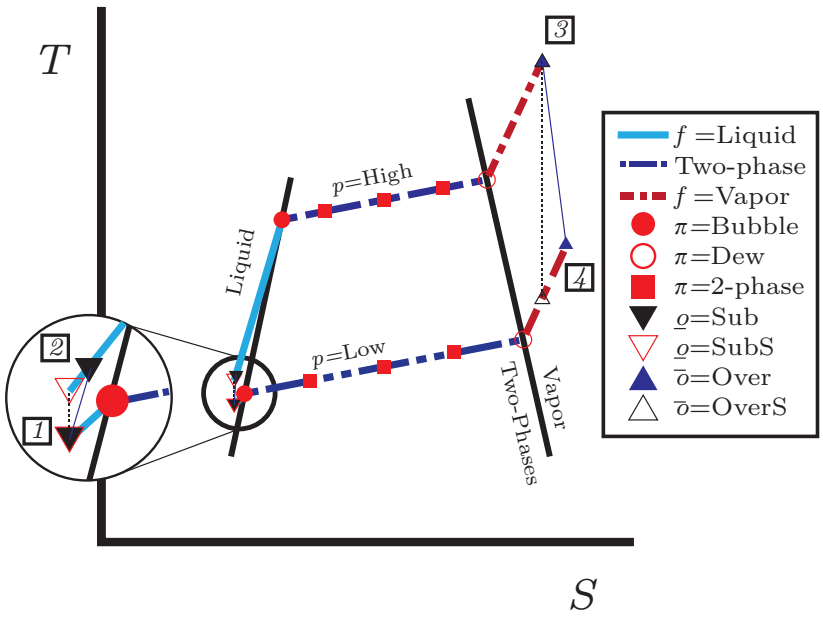

Figure 6: Graphic representation of some of the sets.

equations. It should be remarked that in Figure 7, $\overline{\boldsymbol{U}}_s$ stands for single and series exclusive constraints, and $\overline{\boldsymbol{U}}_s^C$ for the multistage cascade constraints. Note that for Figure 7-(b) there are disjunctive terms which involve the temperature matching equations $\bar{t}_s$

3.2 Objective functions Ω

(1) The maximization of the first law efficiency (η_I)

$$\max_{\overline{\boldsymbol{T}},\overline{\boldsymbol{P}},\overline{\boldsymbol{z}},\overline{\boldsymbol{X}}} \eta_I \tag{1}$$

where $\overline{\boldsymbol{T}}$ stands for the temperatures $T_{s\pi p}$ and TS_{sop}, $\overline{\boldsymbol{P}}$ is the pressure P_{sp}, $\overline{\boldsymbol{z}}$ the compositions z_{is}, and $\overline{\boldsymbol{X}}$ is the rest of variables of the model (e.g. molar flows, thermodynamic properties, etc). The aim of this objective function consists in calculating the operating conditions such that the cycle featuring the largest energy output to heat input ratio(first law efficiency) is designed.

$$
\left.
\begin{array}{c}
\underset{\overline{\boldsymbol{T}},\overline{\boldsymbol{P}},\overline{\boldsymbol{z}},\overline{\boldsymbol{X}}}{\max}\ \Omega \\
\text{s. t.} \quad \overline{\boldsymbol{Z}}_s\left(\overline{\boldsymbol{P}}_s,\overline{\boldsymbol{T}}_s,\overline{\boldsymbol{z}}_s,\overline{\boldsymbol{X}}_s\right)=0 \\
\overline{\boldsymbol{G}}_s\left(\overline{\boldsymbol{P}}_s,\overline{\boldsymbol{T}}_s,\overline{\boldsymbol{z}}_s,\overline{\boldsymbol{X}}_s\right)=0 \\
\overline{\boldsymbol{B}}_d\left(\overline{\boldsymbol{P}}_s,\overline{\boldsymbol{T}}_s,\overline{\boldsymbol{z}}_s,\overline{\boldsymbol{X}}_s\right)=0 \\
\overline{\boldsymbol{\varphi}}_s\left(\overline{\boldsymbol{P}}_s,\overline{\boldsymbol{T}}_s,\overline{\boldsymbol{z}}_s,\overline{\boldsymbol{X}}_s\right)\le 0 \\
\overline{\boldsymbol{C}}_s\left(\overline{\boldsymbol{P}}_s,\overline{\boldsymbol{T}}_s,\overline{\boldsymbol{z}}_s,\overline{\boldsymbol{X}}_s\right)=0 \\
\overline{\boldsymbol{U}}_s\left(\overline{\boldsymbol{P}}_s,\overline{\boldsymbol{T}}_s,\overline{\boldsymbol{z}}_s,\overline{\boldsymbol{X}}_s\right)\le 0 \\
\overline{\boldsymbol{P}}_s,\overline{\boldsymbol{T}}_s\ge 0 \\
0\ge\overline{\boldsymbol{z}}_s\ge 1 \\
\overline{\boldsymbol{P}}_s,\overline{\boldsymbol{T}}_s,\overline{\boldsymbol{z}}_s,\overline{\boldsymbol{X}}_s\in\mathbb{R}^n
\end{array}
\right\} \quad s\in S_{TG}
$$

(a)

$$
\left.
\begin{array}{c}
\underset{\overline{\boldsymbol{T}},\overline{\boldsymbol{P}},\overline{\boldsymbol{z}},\overline{\boldsymbol{X}}}{\max}\ \Omega \\
\text{s. t.} \quad \overline{\boldsymbol{Z}}_s\left(\overline{\boldsymbol{P}}_s,\overline{\boldsymbol{T}}_s,\overline{\boldsymbol{z}}_s,\overline{\boldsymbol{X}}_s\right)=0 \\
\overline{\boldsymbol{G}}_s\left(\overline{\boldsymbol{P}}_s,\overline{\boldsymbol{T}}_s,\overline{\boldsymbol{z}}_s,\overline{\boldsymbol{X}}_s\right)=0 \\
\overline{\boldsymbol{B}}_d\left(\overline{\boldsymbol{P}}_s,\overline{\boldsymbol{T}}_s,\overline{\boldsymbol{z}}_s,\overline{\boldsymbol{X}}_s\right)=0 \\
\overline{\boldsymbol{\varphi}}_s\left(\overline{\boldsymbol{P}}_s,\overline{\boldsymbol{T}}_s,\overline{\boldsymbol{z}}_s,\overline{\boldsymbol{X}}_s\right)\le 0 \\
\overline{\boldsymbol{C}}_s\left(\overline{\boldsymbol{P}}_s,\overline{\boldsymbol{T}}_s,\overline{\boldsymbol{z}}_s,\overline{\boldsymbol{X}}_s\right)=0 \\
\overline{\boldsymbol{U}}_s^{C}\left(\overline{\boldsymbol{P}}_s,\overline{\boldsymbol{T}}_s,\overline{\boldsymbol{z}}_s,\overline{\boldsymbol{X}}_s\right)\le 0 \\
\begin{pmatrix} \hat{Y}_s^{\text{liq}} \\ \bar{t}_s^{L}\,(\text{liq})=0 \end{pmatrix} \vee \begin{pmatrix} \hat{Y}_s^{\text{2P}} \\ \bar{t}_s^{L}\,(\text{2P})=0 \end{pmatrix} \\
\begin{pmatrix} \check{Y}_s^{\text{vap}} \\ \bar{t}_s^{U}\,(\text{vap})=0 \end{pmatrix} \vee \begin{pmatrix} \check{Y}_s^{\text{2P}} \\ \bar{t}_s^{U}\,(\text{2P})=0 \end{pmatrix} \\
\hat{Y}_s^{\text{liq}} \underline{\vee} \hat{Y}_s^{\text{2P}} \\
\check{Y}_s^{\text{vap}} \underline{\vee} \check{Y}_s^{\text{2P}} \\
\overline{\boldsymbol{P}}_s,\overline{\boldsymbol{T}}_s\ge 0 \\
0\ge\overline{\boldsymbol{z}}_s\ge 1 \\
\overline{\boldsymbol{P}}_s,\overline{\boldsymbol{T}}_s,\overline{\boldsymbol{z}}_s,\overline{\boldsymbol{X}}_s\in\mathbb{R}^n \\
\hat{Y}_s^{\text{liq}},\hat{Y}_s^{\text{2P}},\check{Y}_s^{\text{vap}},\check{Y}_s^{\text{2P}}\in\{\text{true,false}\}
\end{array}
\right\} \quad s\in S_{TG}
$$

(b)

Figure 7: Model for the mixture-ORC (a) Single stage ($\overline{\boldsymbol{U}}_s=\overline{\boldsymbol{U}}_s^1, s=1$), and multi-stage series ($\overline{\boldsymbol{U}}_s=\overline{\boldsymbol{U}}_s^S, s\in S_{TG}$). (b) Cascade multi-stage

(2) The minimization of the cost per annual MWh ($\tilde{C}$)

$$\min_{\overline{\boldsymbol{T}},\overline{\boldsymbol{P}},\overline{\boldsymbol{z}},\overline{\boldsymbol{X}}} \tilde{C} \tag{2}$$

This objective function is the ratio between the updated base cost of the cycle plus the overall utilities over its whole lifespan, and the electricity produced in a year (see eq. 184). The aim of using this objective function is to design a cycle whose cost is justified through its energy production. In other words, it implies that whatever cycle is obtained, it would be the one what has the less costly power generation accounting for the operation and fixed cost of the cycle itself.

3.3 Constraints

(1) Equations of state $\overline{\boldsymbol{Z}}_s\left(\overline{\boldsymbol{T}}_s, \overline{\boldsymbol{P}}_s, \overline{\boldsymbol{z}}_s\right) = 0$

A large part of the algebraic model is used to describe the thermodynamics of the cycle by means of equations of state (EOS). The EOS are used in two main forms: for pure components and for mixtures. The thermodynamic behavior of the pure components was described with the Soave-Redlich-Kwong equation of state (SRK) [14]. For mixtures, the Predictive-SRK equation of state (PSRK) [15] was used. This last equation is an extension of the SRK equation for a mixture, with the activity coefficients as part of a mixing rule.

Regarding the notation used in this work, some variables are exclusive of pure components like the temperature functions $(f_T)_{is\pi p}$ or $\alpha_{is\pi p}$, while others are only related to the mixture like $\hat{\alpha}_{s\pi p}$ or $\overline{\alpha}_{is\pi p}$. Additionally, the notation of the equation definitions are simplified. The equations in the form: "variables$_{\text{indexes}}$ =expression" are always defined over: "indexes$\in$Set" (e.g. Eq. 3 with $i \in I, s \in S_{TG}, \pi \in \Pi, p \in L$), except when is explicitly stated in the equation (e.g. $i \in I, s \in S_{TG}, \pi \in \Pi, p \in L$).

The temperature function variables from the SRK EOS for pure at equilibrium, reference and superheat temperatures are as follows:

$$(f_T)_{is\pi p} = \left[1 + c_{\omega,i}\left(1 - (T_{s\pi p}/\mathrm{Tc}_i)^{0.5}\right)\right]^2 \tag{3}$$

$$(\mathrm{fR}_T)_{isp} = \left[1 + c_{\omega,i}\left(1 - (\mathrm{TRF}_{isp}/\mathrm{Tc}_i)^{0.5}\right)\right]^2 \tag{4}$$

$$(\mathrm{fS}_T)_{is\bar{o}p} = \left[1 + c_{\omega,i}\left(1 - (\mathrm{TS}_{s\bar{o}p}/\mathrm{Tc}_i)^{0.5}\right)\right]^2 \tag{5}$$

where $T_{s\pi p}$, TRF_{isp}, and $\mathrm{TS}_{s\bar{o}p}$ are the equilibrium, reference and superheat temperatures. $c_{\omega,i}$ are the acentric parameters and Tc_i are the critical temperatures. The variables for the EOS polynomial are given by the following equations:

$$\alpha_{is\pi p} = \frac{0.42748 R_g \mathrm{Tc}_i^2 \, (f_T)_{is\pi p}}{\mathrm{Pc}_i b_i T_{s\pi p}} \tag{6}$$

$$\mathrm{aR}_{isp} = \frac{0.42748 R_g \mathrm{Tc}_i^2 \, (\mathrm{fR}_T)_{isp}}{\mathrm{Pc}_i b_i \mathrm{TRF}_{isp}} \tag{7}$$

$$\mathrm{aS}_{is\bar{o}p} = \frac{0.42748 R_g \mathrm{Tc}_i^2 \, (\mathrm{fS}_T)_{is\bar{o}p}}{\mathrm{Pc}_i b_i \mathrm{TS}_{s\bar{o}p}} \tag{8}$$

$$\beta^{\mathrm{sat}}_{is\pi p} = \frac{b_i P^{\mathrm{sat}}_{is\pi p}}{R_g T_{s\pi p}} \tag{9}$$

$$\mathrm{bR}_{isp} = \frac{b_i P_{sp}}{R_g \mathrm{TRF}_{isp}} \tag{10}$$

where $P^{\mathrm{sat}}_{is\pi p}$ is the saturation pressure, R_g is the gas constant, Pc_i is the critical pressure and b_i is a pure component parameter. The corresponding mixture variables are the following:

$$\hat{b}_{s\pi p} = \sum_{i \in I} x_{isV\pi p} b_i \tag{11}$$

$$\hat{\beta}_{s\pi p} = \frac{\hat{b}_{s\pi p} P_{sp}}{R_g T_{s\pi p}} \tag{12}$$

$$\hat{\mathrm{bS}}_{s\bar{o}p} = \frac{\hat{b}_{s,\mathrm{Dew},p} P_{sp}}{R_g \mathrm{TS}_{s\bar{o}p}} \tag{13}$$

where $x_{isV\pi p}$ is the equilibrium vapor phase composition and P_{sp} is the cycle pressure. The PSRK (Predictive-SRK) mixing rule involves the compositions and the Gibbs excess energy of the mixture $G_{s\pi Vp}$ (and $\mathrm{GS}_{s\bar{o}p}$ for superheat) given by the activity coefficients.

$$\hat{\alpha}_{s\pi p} = -\frac{1}{0.64663}\left(G_{s\pi Vp} + \sum_{i\in I} x_{isV\pi p} \ln \frac{\hat{b}_{s\pi p}}{b_i}\right) + \sum_{i\in I} x_{isV\pi p}(\alpha_{is\pi p}) \tag{14}$$

$$\hat{\mathrm{aS}}_{s\bar{o}p} = -\frac{1}{0.64663}\left(\mathrm{GS}_{s\bar{o}p} + \sum_{i\in I} z_{is} \ln \frac{\hat{b}_{s,\mathrm{Dew},p}}{b_i}\right) + \sum_{i\in I} z_{is}(\mathrm{aS}_{is\bar{o}p}) \tag{15}$$

Considering that $\hat{\mathrm{aS}}_{s\bar{o}p}$ is at nonphase-equilibrium conditions, the global composition z_{is} is then used. Also the molar partial variable is given by,

$$\overline{\alpha}_{is\pi p} = \frac{1}{\mathrm{A1}}\left(\ln \gamma_{is\pi Vp} + \ln \frac{\hat{\beta}_{s\pi p}}{\beta_i} + \frac{\beta_{is\pi p}}{\hat{\beta}_{s\pi p}} - 1\right) + \alpha_{is\pi p} \tag{16}$$

where $\ln \gamma_{is\pi Vp}$ is the activity coefficient with the composition of the vapor phase and A1 is a parameter. Next, the constraints that are related to the compressibility factor variable are cubic polynomials. Each one of these constraints is related to a required state, namely pure saturation, reference temperature, mixture at equilibrium and nonequilibrium.

$$\left(Z^{\mathrm{sat}}_{is\pi p}\right)^3 - \left(Z^{\mathrm{sat}}_{is\pi p}\right)^2 + \left[-\beta^{\mathrm{sat}}_{is\pi p} - \left(\beta^{\mathrm{sat}}_{is\pi p}\right)^2 + \alpha_{is\pi p}\beta^{\mathrm{sat}}_{is\pi p}\right] Z^{\mathrm{sat}}_{is\pi p} - \alpha_{is\pi p}\left(\beta^{\mathrm{sat}}_{is\pi p}\right)^2 = 0 \qquad i \in I, s \in S_{TG}, \pi \in \Pi, p \in L \tag{17}$$

$$\left(\mathrm{ZR}_{isp}\right)^3 - \left(\mathrm{ZR}_{isp}\right)^2 + \left[-\mathrm{bR}_{isp} - \left(\mathrm{bR}_{isp}\right)^2 + \mathrm{aR}_{isp}\mathrm{bR}_{isp}\right] \mathrm{ZR}_{isp} - \mathrm{aR}_{isp}\left(\mathrm{bR}_{isp}\right)^2 = 0, \qquad i \in I, s \in S_{TG}, p \in L \tag{18}$$

$$\left(\hat{Z}_{s\pi p}\right)^3 - \left(\hat{Z}_{s\pi p}\right)^2 + \left[-\hat{\beta}_{s\pi p} - \left(\hat{\beta}_{s\pi p}\right)^2 + \hat{\alpha}_{s\pi p}\hat{\beta}_{s\pi p}\right] \hat{Z}_{s\pi p} - \hat{\alpha}_{s\pi p}\left(\hat{\beta}_{s\pi p}\right)^2 = 0, \qquad s \in S_{TG}, \pi \in \Pi, p \in L \tag{19}$$

$$\left(\hat{\mathrm{ZS}}_{s\bar{o}p}\right)^3 - \left(\hat{\mathrm{ZS}}_{s\bar{o}p}\right)^2 + \left[-\hat{\mathrm{bS}}_{s\bar{o}p} - \left(\hat{\mathrm{bS}}_{s\bar{o}p}\right)^2 + \hat{\mathrm{aS}}_{s\bar{o}p}\hat{\mathrm{bS}}_{s\bar{o}p}\right]\hat{\mathrm{ZS}}_{s\bar{o}p} - \hat{\mathrm{aS}}_{s\bar{o}p}\left(\hat{\mathrm{bS}}_{s\bar{o}p}\right)^2 = 0,$$
$$s \in S_{TG}, \bar{o} \in \overline{O}, p \in L \tag{20}$$

where $Z^{\mathrm{sat}}_{is\pi p}, \mathrm{ZR}_{isp}, \hat{Z}_{s\pi p}$ and $\hat{\mathrm{ZS}}_{s\bar{o}p}$ are the respective compressibility factors. It should be noted that because the previous equations are cubic polynomials, more than one root is expected. Only one is useful for our purposes (i.e. the vapor root). Therefore, we require a way of discerning which of the roots are we obtaining at the same time that the problem is being solved. This is problematic; however a simple yet convenient method for dealing with this issue is by adding the two constraints introduced in [16]. These two constraints involve the first and second derivatives of the previous equations. Then, the first derivative constraints are:

$$3\left(Z^{\mathrm{sat}}_{is\pi p}\right)^2 - 2Z^{\mathrm{sat}}_{is\pi p} + \left[-\beta^{\mathrm{sat}}_{is\pi p} - \left(\beta^{\mathrm{sat}}_{is\pi p}\right)^2 + \alpha_{is\pi p}\beta^{\mathrm{sat}}_{is\pi p}\right] \geq 0,$$
$$i \in I, s \in S_{TG}, \pi \in \Pi, p \in L \tag{21}$$

$$3\left(\hat{Z}_{s\pi p}\right)^2 - 2\hat{Z}_{s\pi p} + \left[-\hat{\beta}_{s\pi p} - \left(\hat{\beta}_{s\pi p}\right)^2 + \hat{\alpha}_{s\pi p}\hat{\beta}_{s\pi p}\right] \geq 0,$$
$$s \in S_{TG}, \pi \in \Pi, p \in L \tag{22}$$

$$3\left(\mathrm{ZR}_{isp}\right)^2 - 2\mathrm{ZR}_{isp} + \left[-\mathrm{bR}_{isp} - \left(\mathrm{bR}_{isp}\right)^2 + \mathrm{aR}_{isp}\mathrm{bR}_{isp}\right] \geq 0,$$
$$i \in I, s \in S_{TG}, p \in L \tag{23}$$

$$3\left(\hat{\mathrm{ZS}}_{s\bar{o}p}\right)^2 - 2\hat{\mathrm{ZS}}_{s\bar{o}p} + \left[-\hat{\mathrm{bS}}_{s\bar{o}p} - \left(\hat{\mathrm{bS}}_{s\bar{o}p}\right)^2 + \hat{\mathrm{aS}}_{s\bar{o}p}\hat{\mathrm{bS}}_{s\bar{o}p}\right] \geq 0,$$
$$s \in S_{TG}, \bar{o} \in \overline{O}, p \in L \tag{24}$$

And the second derivative constraints:

$$6\left(Z^{\mathrm{sat}}_{is\pi p}\right) - 2 \geq 0, \quad i \in I, s \in S_{TG}, \pi \in \Pi, p \in L \tag{25}$$

$$6\left(\hat{Z}_{s\pi p}\right) - 2 \geq 0, \quad s \in S_{TG}, \pi \in \Pi, p \in L \tag{26}$$

$$6\left(\mathrm{ZR}_{isp}\right) - 2 \geq 0, \quad i \in I, s \in S_{TG}, \pi \in \Pi, p \in L \tag{27}$$

$$6\left(\hat{\mathrm{Z}}\mathrm{S}_{s\bar{o}p}\right) - 2 \geq 0, \quad s \in S_{TG}, \overline{o} \in \overline{O}, p \in L \tag{28}$$

These equations collectively will allow us to obtain an appropriate root for the compressibility factor.

(2) Activity Coefficients $\overline{\boldsymbol{G}}_s\left(\overline{\boldsymbol{T}}_s, \overline{\boldsymbol{P}}_s, \overline{\boldsymbol{z}}_s, \overline{\boldsymbol{X}}\right) = 0$

The versatility of the UNIFAC [17] method makes it appropriate for this model, since it does not require pure component experimental information, just the binary interaction parameters for each functional group pair in the mixture, and two additional parameter for each group. The only disadvantage is that it depends on binary interaction parameters a_{mn}.

The following equations are the core of the UNIFAC activity coefficients model.

$$\ln \gamma_{is\pi fp} = \ln \gamma^{C}_{is\pi fp} + \ln \gamma^{R}_{is\pi fp} \tag{29a}$$

$$\ln \gamma^{C}_{is\pi fp} = \ln \frac{r_i}{\sum\limits_{j\in I} r_j x_{js\pi fp}} + \frac{10}{2} q_i \ln \frac{q_i \sum\limits_{j\in I} r_j x_{js\pi fp}}{r_i \sum\limits_{j\in I} q_j x_{js\pi fp}} + l_i - \frac{r_i}{\sum\limits_{j\in I} r_j x_{js\pi fp}} \sum_{j\in I} x_{js\pi fp} l_j \tag{29b}$$

$$\ln \gamma^{R}_{is\pi fp} = \sum_{k\in M} \nu_{ik} \left(\ln \Gamma_{ks\pi fp} - \mathrm{lGP}_{iks\pi p}\right) \tag{29c}$$

$$\mathrm{lGP}_{iks\pi p} = Q_k \left[1 - \ln\left(\sum_{m\in M} \mathrm{TP}_{im} \Psi_{mks\pi p}\right) - \sum_{m\in M} \frac{\mathrm{TP}_{im} \Psi_{kms\pi p}}{\sum\limits_{n\in M} \mathrm{TP}_{in} \Psi_{nms\pi p}}\right] \tag{29d}$$

$$\ln \Gamma_{ks\pi fp} = Q_k \left[1 - \ln\left(\sum_{m\in M} \theta_{ms\pi fp} \Psi_{mks\pi p}\right) - \sum_{m\in M} \frac{\theta_{ms\pi fp} \Psi_{kms\pi p}}{\sum\limits_{n\in M} \theta_{ns\pi fp} \Psi_{nms\pi p}}\right] \tag{29e}$$

$$\theta_{ms\pi fp} = \frac{Q_m X_{ms\pi fp}}{\sum\limits_{n\in M} Q_n X_{ns\pi fp}} \tag{29f}$$

$$\Psi_{mns\pi p} = \exp\left(-\frac{a_{mn}}{T_{s\pi p}}\right) \tag{29g}$$

$$X_{ms\pi fp} = \frac{\sum\limits_{i\in I} x_{is\pi fp}\nu_{im}}{\sum\limits_{i\in I}\left(x_{is\pi fp}\sum\limits_{n\in M}\nu_{in}\right)} \tag{29h}$$

The required parameters are:

$$r_i = \sum_{k\in M} \nu_{ik} R_k \tag{30a}$$

$$q_i = \sum_{k\in M} \nu_{ik} Q_k \tag{30b}$$

$$l_i = \frac{10}{2}(r_i - q_i) - (r_i - 1) \tag{30c}$$

$$\mathrm{TP}_{im} = \frac{Q_m \mathrm{XP}_{im}}{\sum\limits_{n\in M} Q_n \mathrm{XP}_{in}} \tag{30d}$$

$$\mathrm{XP}_{im} = \frac{\nu_{im}}{\sum\limits_{n\in M}\nu_{in}} \tag{30e}$$

where ν_{im} is the group frequency, a_{mn} [18] is the binary interaction parameter, R_k and Q_k are group parameters. We only display the group for UNIFAC once, but in fact the equations are required one second time with the temperature TS*sop*. Also, through this work, the temperature derivatives of the activity coefficient are required. But they only involve the temperature dependent variables, namely the equations with $\Psi_{mns\pi p}$. We will not show them but the derivation is straightforward and can be found elsewhere [19].

(3) Equilibrium and Property constraints $\overline{\boldsymbol{B}}_s\left(\overline{\boldsymbol{T}}_s, \overline{\boldsymbol{P}}_s, \overline{\boldsymbol{z}}_s, \overline{\boldsymbol{X}}\right) = 0$

(a) Equilibrium. The equilibrium constraints consist of equalities involving fugacity coefficients, K-value and the Rachford-Rice equation. These equations are only defined for the two-phase region of the cycle, i.e. inside the heat exchangers. First, the fugacity coefficient constraints are defined for the pure species at saturation pressure and the mixture at equilibrium temperature [20].

$$\left(\ln \Phi^{\text{sat}}\right)_{is\pi p} = Z^{\text{sat}}_{is\pi p} - 1 - \ln\left(Z^{\text{sat}}_{is\pi p} - \beta^{\text{sat}}_{is\pi p}\right) - \alpha_{is\pi p} \ln\left(\frac{Z^{\text{sat}}_{is\pi p} + \beta^{\text{sat}}_{is\pi p}}{Z^{\text{sat}}_{is\pi p}}\right) \tag{31}$$

$$\left(\ln \hat{\Phi}\right)_{is\pi p} = \frac{b_i}{\hat{b}_{s\pi p}}\left(\hat{Z}_{s\pi p} - 1\right) - \ln\left(\hat{Z}_{s\pi p} - \hat{\beta}_{s\pi p}\right) - \overline{\alpha}_{is\pi p} \ln\left(\frac{\hat{Z}_{s\pi p} + \beta_{s\pi p}}{\hat{Z}_{s\pi p}}\right) \tag{32}$$

The K-value or equilibrium ratio as given here assumes incompressible liquids. Also the inclusion of the activity coefficient of the liquid phase ($\ln \gamma_{is\pi Lp}$) has to be noted:

$$K_{is\pi p} = \frac{\exp\left(\ln \gamma_{is\pi Lp}\right) P^{\text{sat}}_{is\pi p} \exp\left(\ln \Phi^{\text{sat}}\right)_{is\pi p}}{\exp\left(\ln \hat{\Phi}\right)_{is\pi p} P_{sp}} \tag{33}$$

Regarding the Rachford-Rice equation [21] a re-arranged version of the equation was used because the original form is prone to becoming undefined during the solution process:

$$\sum_{i \in I}\left(\frac{z_{is}}{1 + \psi_\pi\left(K_{is\pi p} - 1\right)} \prod_{j \in I}\left(1 + \psi_\pi\left(K_{js\pi p} - 1\right)\right)\right) = 0 \qquad s \in S_{TG}, \pi \in \Pi, p \in L \tag{34}$$

where ψ_π is the vapor phase ratio. With the equilibrium constraints now defined, the last constraints are the mole fraction of the vapor, liquid and consistency equations. For the liquid phase:

$$x_{isL\pi p} = \frac{z_{is}}{\left(1 + \psi_\pi\left(K_{is\pi p} - 1\right)\right)} \tag{35}$$

whereas for the vapor phase:

$$x_{isV\pi p} = \frac{z_{is} K_{is\pi p}}{(1 + \psi_\pi (K_{is\pi p} - 1))} \tag{36}$$

and the summations consistency equations:

$$\sum_{i \in I} z_{is} = 1, \quad i \in I \tag{37}$$

$$\sum_{i \in I} x_{isf\pi p} = 1, \quad i \in I, s \in S_{TG}, \pi \in \Pi, p \in L \tag{38}$$

(b) Property. The property section of the model deals with the constraints for the vapor pressure, reference temperature, enthalpy and entropy; these last two being the most important because they allow us to know the thermodynamic states over the cycle and the overall energy inputs and outputs.

The vapor pressure (or saturation) and the reference temperature are each one given by the extended Antoine equation [22]:

$$\ln P^{\text{sat}}_{is\pi p} = C_{1,i} - \frac{C_{2,i}}{T_{is\pi p} + C_{3,i}} + C_{4,i} T_{is\pi p} + C_{5,i} \ln T_{is\pi p} + C_{6,i} T^{C_{7,i}}_{is\pi p} \tag{39}$$

$$\ln P_{sp} = C_{1,i} - \frac{C_{2,i}}{\text{TRF}_{is\pi p} + C_{3,i}} + C_{4,i} \text{TRF}_{is\pi p} + C_{5,i} \ln \text{TRF}_{is\pi p} + C_{6,i} \text{TRF}^{C_{7,i}}_{is\pi p} \tag{40}$$

The first equation gives the saturation pressure $P^{\text{sat}}_{is\pi p}$ for the equilibrium temperature $T_{is\pi p}$, whereas the second one gives the reference temperature $\text{TRF}_{is\pi p}$ for the pressure of the cycle P_{sp}. Moreover, $C_{1,i}$ through $C_{7,i}$ are parameters for the pure species. These parameters were taken from the Aspen Plus property data [23].

The enthalpy and entropy are established for the liquid and vapor phases through the residuals (or departures from ideal gas), ideal gas and liquid changes, and the latent heat. First, the residuals require temperature derivatives of the parameters used in the EOS

section.

$$(f'_T)_{isp} = -\frac{c_{\omega,i}}{\mathrm{Tc}_i}\left[1 + c_{\omega,i}\left(1 - (T_{s,\mathrm{Dew},p}/\mathrm{Tc}_i)^{0.5}\right)\right]\left(\frac{T_{s,\mathrm{Dew},p}}{\mathrm{Tc}_i}\right)^{-0.5} \tag{41}$$

$$(\mathrm{fR}'_T)_{isp} = -\frac{c_{\omega,i}}{\mathrm{Tc}_i}\left[1 + c_{\omega,i}\left(1 - (\mathrm{TRF}_{isp}/\mathrm{Tc}_i)^{0.5}\right)\right]\left(\frac{\mathrm{TRF}_{isp}}{\mathrm{Tc}_i}\right)^{-0.5} \tag{42}$$

$$(\mathrm{fS}'_T)_{is\bar{o}p} = -\frac{c_{\omega,i}}{\mathrm{Tc}_i}\left[1 + c_{\omega,i}\left(1 - (\mathrm{TS}_{s\bar{o}p}/\mathrm{Tc}_i)^{0.5}\right)\right]\left(\frac{\mathrm{TS}_{s\bar{o}p}}{\mathrm{Tc}_i}\right)^{-0.5} \tag{43}$$

$$\mathrm{aR}'_{isp} = 0.42748\,(\mathrm{fR}'_T)_{isp} \tag{44}$$

$$a'_{isp} = 0.42748\,(f'_T)_{isp} \tag{45}$$

$$\mathrm{aS}'_{is\bar{o}p} = 0.42748\,(\mathrm{fS}'_T)_{is\bar{o}p} \tag{46}$$

The temperature derivatives of the mixture variables are related to the Gibbs excess energy derivatives G'_{sp} and $\mathrm{GS}'_{s\bar{o}p}$.

$$\hat{a}'_{sp} = \frac{G'_{sp}}{\mathrm{A1}} + \left(\sum_{i\in I} z_{is}\frac{a'_{isp}}{b_i}\frac{R_g^2\mathrm{Tc}_i^2}{\mathrm{Pc}_i}\right) + \frac{R_g}{\mathrm{A1}}\sum_{i\in I} z_{is}\ln\left(\frac{\hat{b}_{s,\mathrm{Dew},p}}{b_i}\right) \tag{47}$$

$$\hat{\mathrm{a}}\mathrm{S}'_{s\bar{o}p} = \frac{\mathrm{GS}'_{s\bar{o}p}}{\mathrm{A1}} + \left(\sum_{i\in I} z_{is}\frac{\mathrm{aS}'_{is\bar{o}p}}{b_i}\frac{R_g^2\mathrm{Tc}_i^2}{\mathrm{Pc}_i}\right) + \frac{R_g}{\mathrm{A1}}\sum_{i\in I} z_{is}\ln\left(\frac{\hat{b}_{s,\mathrm{Dew},p}}{b_i}\right) \tag{48}$$

The enthalpy ($\left(H^R\right)_{sp}$, HRRF_{isp} and $(\mathrm{HR})_{s\bar{o}p}$) and entropy ($\left(S^R\right)_{sp}$, SRRF_{isp} and $(\mathrm{SR})_{s\bar{o}p}$) residual equations [20] are defined for assessing the phase equilibrium behavior, the reference state and the superheat states. Enthalpy:

$$\left(H^R\right)_{sp} = -\left(\hat{\alpha}_{s,\mathrm{Dew},p} - \frac{\hat{a}'_{sp}}{R_g}\right)\ln\frac{\hat{Z}_{s,\mathrm{Dew},p}}{\hat{Z}_{s,\mathrm{Dew},p} + \hat{\beta}_{s,\mathrm{Dew},p}} + 1 - \hat{Z}_{s,\mathrm{Dew},p} \tag{49}$$

$$\mathrm{HRRF}_{isp} = -\left(\mathrm{aR}_{isp} - \frac{\mathrm{aR}'_{isp}R_g\mathrm{Tc}_i^2}{\mathrm{Pc}_i b_i}\right)\ln\frac{\mathrm{ZR}_{isp}}{\mathrm{ZR}_{isp} + \mathrm{bR}_{isp}} + 1 - \mathrm{ZR}_{isp} \tag{50}$$

$$(\mathrm{HR})_{s\bar{o}p} = -\left(\hat{\mathrm{a}}\mathrm{S}_{s\bar{o}p} - \frac{\hat{\mathrm{a}}\mathrm{S}'_{s\bar{o}p}}{R_g}\right)\ln\frac{\hat{\mathrm{Z}}\mathrm{S}_{s\bar{o}p}}{\hat{\mathrm{Z}}\mathrm{S}_{s\bar{o}p} + \hat{\mathrm{b}}\mathrm{S}_{s\bar{o}p}} + 1 - \hat{\mathrm{Z}}\mathrm{S}_{s\bar{o}p} \tag{51}$$

Entropy:

$$\left(S^R\right)_{sp} = -\ln\left(\hat{Z}_{s,\mathrm{Dew},p} - \hat{\beta}_{s,\mathrm{Dew},p}\right) + \frac{\hat{a}'_{s,\mathrm{Dew},p}}{R_g}\ln\frac{\hat{Z}_{s,\mathrm{Dew},p}}{\hat{Z}_{s,\mathrm{Dew},p} + \hat{\beta}_{s,\mathrm{Dew},p}} \tag{52}$$

$$\mathrm{SRRF}_{isp} = -\ln\left(\mathrm{ZR}_{isp} - \mathrm{bR}_{isp}\right) + \frac{\mathrm{aR}'_{isp} R_g \mathrm{Tc}_i^2}{\mathrm{Pc}_i b_i}\ln\frac{\mathrm{ZR}_{isp}}{\mathrm{ZR}_{isp} + \mathrm{bR}_{isp}} \tag{53}$$

$$\left(\mathrm{SR}\right)_{s\bar{o}p} = -\ln\left(\hat{\mathrm{Z}}\mathrm{S}_{s\bar{o}p} - \hat{\beta}_{s,\mathrm{Dew},p}\right) + \frac{\hat{\mathrm{a}}\mathrm{S}'_{s\bar{o}p}}{R_g}\ln\frac{\hat{\mathrm{Z}}\mathrm{S}_{s\bar{o}p}}{\hat{\mathrm{Z}}\mathrm{S}_{s\bar{o}p} + \hat{\mathrm{b}}\mathrm{S}_{s\bar{o}p}} \tag{54}$$

Note that the residuals are given in terms of temperature derivatives of the SRK and PSRK variables and the compressibility factor. For the definition of the properties we also need the ideal gas changes. Both use equations with parameters fitted from the integrated form of an equation used in [8]. This leaves consistently simple equations, although the accuracy of the predicted change values is reduced. Once again three states are evaluated, so three equations for each property are required.

Enthalpy:

$$\begin{aligned}&\mathrm{Hu}\left(\mathrm{DHR}^{id}\right)_{isp} = \\ &\frac{\mathrm{cpx1}_i}{3}\left[\left(\mathrm{TRF}_{isp}\right)^3 - 298.15^3\right] + \frac{\mathrm{cpx2}_i}{2}\left[\left(\mathrm{TRF}_{isp}\right)^2 - 298.15^2\right] + \mathrm{cpx3}_i\left[\mathrm{TRF}_{isp} - 298.15\right]\end{aligned} \tag{55}$$

$$\begin{aligned}&\mathrm{Hu}\left(\Delta H^{id}\right)_{isp} = \\ &\frac{\mathrm{cpx1}_i}{3}\left[\left(T_{s,\mathrm{Dew},p}\right)^3 - 298.15^3\right] + \frac{\mathrm{cpx2}_i}{2}\left[\left(T_{s,\mathrm{Dew},p}\right)^2 - 298.15^2\right] + \mathrm{cpx3}_i\left[T_{s,\mathrm{Dew},p} - 298.15\right]\end{aligned} \tag{56}$$

$$\begin{aligned}&\mathrm{Hu}\left(\Delta\mathrm{Hs}\right)_{is\bar{o}p} = \\ &\frac{\mathrm{cpx1}_i}{3}\left[\left(\mathrm{TS}_{s\underline{o}p}\right)^3 - 298.15^3\right] + \frac{\mathrm{cpx2}_i}{2}\left[\left(\mathrm{TS}_{s\underline{o}p}\right)^2 - 298.15^2\right] + \mathrm{cpx3}_i\left[\mathrm{TS}_{s\underline{o}p} - 298.15\right]\end{aligned} \tag{57}$$

Entropy:

$$\mathrm{Su}\left(\mathrm{sTR}^{id}\right)_{isp} = \frac{\mathrm{cpx1}_i}{2}\left[\left(\mathrm{TRF}_{isp}\right)^2 - 298.15^2\right] + \mathrm{cpx2}_i\left[\mathrm{TRF}_{isp} - 298.15\right] + \mathrm{cpx3}_i\left[\ln\left(\mathrm{TRF}_{isp}\right) - \ln 298.15\right] \tag{58}$$

$$\mathrm{Su}\left(\Delta S^{id}\right)_{isp} = \frac{\mathrm{cpx1}_i}{2}\left[\left(T_{s,\mathrm{Dew},p}\right)^2 - 298.15^2\right] + \mathrm{cpx2}_i\left[T_{s,\mathrm{Dew},p} - 298.15\right] + \mathrm{cpx3}_i\left[\ln\left(T_{s,\mathrm{Dew},p}\right) - \ln 298.15\right] \tag{59}$$

$$\mathrm{Su}\left(\Delta \mathrm{Ss}\right)_{is\bar{o}p} = \frac{\mathrm{cpx1}_i}{2}\left[\left(\mathrm{TS}_{s\underline{o}p}\right)^2 - 298.15^2\right] + \mathrm{cpx2}_i\left[\mathrm{TS}_{s\underline{o}p} - 298.15\right] + \mathrm{cpx3}_i\left[\ln\left(\mathrm{TS}_{s\underline{o}p}\right) - \ln 298.15\right] \tag{60}$$

where the parameters $\mathrm{cpx1}_i$ through $\mathrm{cpx3}_i$ are reported in the results section. It has to be noted that the parameters Hu and Su were also added as scaling factors in all enthalpy equations. We also implemented this last technique for the liquid property changes. This time the pure parameters $\mathrm{cpl1}_i$ to $\mathrm{cpl3}_i$ were used. Enthalpy:

$$\mathrm{Hu}\left(\Delta \mathrm{Hl}_{isp}\right) = \frac{\mathrm{cpl1}_i}{3}\left[\left(T_{s,\mathrm{Bubl},p}\right)^3 - \mathrm{TRF}_{isp}^3\right] + \frac{\mathrm{cpl2}_i}{2}\left[\left(T_{s,\mathrm{Bubl},p}\right)^2 - \mathrm{TRF}_{isp}^2\right] + \mathrm{cpl3}_i\left[T_{s,\mathrm{Bubl},p} - \mathrm{TRF}_{isp}\right] \tag{61}$$

$$\mathrm{Hu}\left(\Delta \mathrm{HlS}_{is\underline{o}p}\right) = \frac{\mathrm{cpl1}_i}{3}\left[\left(\mathrm{TS}_{s\underline{o}p}\right)^3 - \mathrm{TRF}_{isp}^3\right] + \frac{\mathrm{cpl2}_i}{2}\left[\left(\mathrm{TS}_{s\underline{o}p}\right)^2 - \mathrm{TRF}_{isp}^2\right] + \mathrm{cpl3}_i\left[\mathrm{TS}_{s\underline{o}p} - \mathrm{TRF}_{isp}\right] \tag{62}$$

Entropy:

$$\mathrm{Su}\left(\Delta \mathrm{Sl}_{isp}\right) = \frac{\mathrm{cpl1}_i}{2}\left[\left(T_{s,\mathrm{Bubl},p}\right)^2 - \mathrm{TRF}_{isp}^2\right] + \mathrm{cpl2}_i\left[T_{s,\mathrm{Bubl},p} - \mathrm{TRF}_{isp}\right] + \mathrm{cpl3}_i\left[\ln\left(T_{s,\mathrm{Bubl},p}\right) - \ln \mathrm{TRF}_{isp}\right] \tag{63}$$

$$\mathrm{Su}\left(\Delta \mathrm{SlS}_{is\underline{o}p}\right) = \frac{\mathrm{cpl1}_i}{2}\left[\left(\mathrm{TS}_{s\underline{o}p}\right)^2 - \mathrm{TRF}_{isp}^2\right] + \mathrm{cpl2}_i\left[\mathrm{TS}_{s\underline{o}p} - \mathrm{TRF}_{isp}\right] + \mathrm{cpl3}_i\left[\ln\left(\mathrm{TS}_{s\underline{o}p}\right) - \ln \mathrm{TRF}_{isp}\right] \tag{64}$$

Only two states for the liquid phase are needed (i.e. equilibrium and nonequilibrium).

Reference vaporization enthalpy (latent heat) equation through the Watson equation [14]:

$$\left(\mathrm{DhR}^{\mathrm{lv}}\right)_{isp} = \Delta \mathrm{hB}_i^{\mathrm{LV}}\left(\frac{1 - \mathrm{TRF}_{isp}/\mathrm{Tc}_i}{1 - \mathrm{Tbr}_i}\right)^{0.375} \tag{65}$$

Those constraints lead to the definition of the molar properties. In the case of the liquid phase, start from the formation enthalpy and Gibbs free energy (DHF_i and $\mathrm{DGF}i$) of the pure species at ideal gas state with 298.15 K and 1 atm. Then the changes go from pure ideal to real gas, pressure correction, condensation at the reference temperature, ideal liquid solution to real liquid solution, and liquid change to the final temperature ($T_{s,\mathrm{Bubl},p}$ or $\mathrm{TS}_{s\underline{o}p}$). All these steps of calculation are embedded in the following 4 equations for the liquid phase enthalpy and entropy.

Enthalpy:

$$h_{sp} = \sum_{i \in I} z_{is}\left[\frac{\mathrm{DHF}_i}{\mathrm{Hu}} + \left(\mathrm{DHR}^{id}\right)_{isp} - \frac{8.314}{\mathrm{Hu}}\mathrm{TRF}_{isp}\mathrm{HRRF}_{isp} - \left(\mathrm{DhR}^{\mathrm{lv}}\right)_{isp} + \Delta \mathrm{Hl}_{isp}\right] \tag{66}$$

$$\mathrm{hS}_{s\underline{o}p} = \sum_{i \in I} z_{is}\left[\frac{\mathrm{DHF}_i}{\mathrm{Hu}} + \left(\mathrm{DHR}^{id}\right)_{isp} - \frac{8.314}{\mathrm{Hu}}\mathrm{TRF}_{isp}\mathrm{HRRF}_{isp} - \left(\mathrm{DhR}^{\mathrm{lv}}\right)_{isp} + \Delta \mathrm{HlS}_{is\underline{o}p}\right] \tag{67}$$

Entropy:

$$s_{sp} = \sum_{i \in I} z_{is} \left[\frac{\mathrm{DHF}_i - \mathrm{DGF}_i}{\mathrm{Su} \cdot 298.15} + \left(\mathrm{sR}^{id}\right)_{isp} - \frac{8.314}{\mathrm{Su}} \left[\ln\left(\frac{P_{sp}}{1.01325}\right) + \mathrm{SRRF}_{isp} \right] - \frac{\mathrm{Hu}}{\mathrm{Su}} \frac{\left(\mathrm{DhR}^{\mathrm{lv}}\right)_{isp}}{\mathrm{TRF}_{isp}} + \Delta\mathrm{Sl}_{isp} \right] \tag{68}$$

$$\mathrm{sS}_{s\underline{o}p} = \sum_{i \in I} z_{is} \cdot \left[\frac{\mathrm{DHF}_i - \mathrm{DGF}_i}{\mathrm{Su} \cdot 298.15} + \left(\mathrm{sR}^{id}\right)_{isp} - \frac{8.314}{\mathrm{Su}} \ln\left(\frac{P_{sp}}{1.01325}\right) + \frac{8.314}{\mathrm{Su}} \mathrm{SRRF}_{isp} - \frac{\mathrm{Hu}}{\mathrm{Su}} \frac{\left(\mathrm{DhR}^{\mathrm{lv}}\right)_{isp}}{\mathrm{TRF}_{isp}} + \Delta\mathrm{SlS}_{is\underline{o}p} \right] \tag{69}$$

The vapor phase properties follow a shorter trajectory, from ideal gas at 298.15 K and 1 atm, ideal gas change, pressure change, and ideal gas mixture to real gas mixture. The gas enthalpy is given by:

$$H_{sp} = \sum_{i \in I} z_{is} \left[\frac{\mathrm{DHF}_i}{\mathrm{Hu}} + \left(\Delta H^{id}\right)_{isp} \right] - \left(H^R\right)_{sp} T_{s,\mathrm{Dew},p} \frac{8.314}{\mathrm{Hu}} \tag{70}$$

$$\mathrm{HS}_{s\bar{o}p} = \sum_{i \in I} z_{is} \left[\frac{\mathrm{DHF}_i}{\mathrm{Hu}} + \left(\Delta\mathrm{Hs}\right)_{is\bar{o}p} \right] - \left(\mathrm{HR}\right)_{s\bar{o}p} \mathrm{TS}_{s\bar{o}p} \frac{8.314}{\mathrm{Hu}} \tag{71}$$

while the gas entropy by,

$$S_{sp} = \sum_{i \in I} z_{is} \left[\frac{\mathrm{DHF}_i - \mathrm{DGF}_i}{\mathrm{Su} \cdot 298.15} + \left(\Delta S^{id}\right)_{isp} - \frac{8.314}{\mathrm{Su}} \ln\left(\frac{P_{sp}}{1.01325}\right) \right] - \left(S^R\right)_{sp} \frac{8.314}{\mathrm{Su}} \tag{72}$$

$$\mathrm{SS}_{s\bar{o}p} = \sum_{i \in I} z_{is} \left[\frac{\mathrm{DHF}_i - \mathrm{DGF}_i}{\mathrm{Su} \cdot 298.15} + \left(\Delta\mathrm{Ss}\right)_{is\bar{o}p} - \frac{8.314}{\mathrm{Su}} \ln\left(\frac{P_{sp}}{1.01325}\right) \right] - \left(\mathrm{SR}\right)_{s\bar{o}p} \frac{8.314}{\mathrm{Su}} \tag{73}$$

It should be noted that the units of the enthalpy and entropy are relative to the value of the factors Hu and Su.

(4) Operation constraints $\overline{\varphi}_s\left(\overline{\boldsymbol{P}}_s, \overline{\boldsymbol{T}}_s, \overline{\boldsymbol{z}}_s, \overline{\boldsymbol{X}}\right) \leq 0$

These constraints take into account the physical pressure and temperature restrictions of the model, compression and expansion properties, and mole ratios.

Pressure level constraint:

$$P_{s,\text{High}} - P_{s,\text{Low}} \geq 0.1, \quad s \in S_{TG} \tag{74}$$

Operation strictly under the critical temperatures (Tc_i):

$$\frac{T_{s\pi p}}{\text{Tc}_i} \leq 0.9999, \quad s \in S_{TG}, \pi \in \Pi, p \in L \tag{75}$$

$$\frac{\text{TS}_{sop}}{\text{Tc}_i} \leq 0.9999, \quad s \in S_{TG}, o \in O, p \in L \tag{76}$$

Temperature consistency:

$$\text{TS}_{s,\text{Over},p} - T_{s,\text{Dew},p} \geq 0, \quad s \in S_{TG}, p \in L \tag{77}$$

$$T_{s,\text{Bubl},p} - \text{TS}_{s,\text{Sub},p} \geq 0, \quad s \in S_{TG}, p \in L \tag{78}$$

$$\text{TS}_{s\underline{o},\text{High}} - \text{TS}_{s\underline{o},\text{Low}} \geq 0, \quad s \in S_{TG}, \underline{o} \in \underline{O} \tag{79}$$

$$T_{s\pi,\text{High}} - T_{s\pi,\text{Low}} \geq 0, \quad s \in S_{TG}, \pi \in \Pi \tag{80}$$

Entropy consistency:

$$\text{SS}_{s,\text{Over},p} - S_{sp} \geq 0, \quad s \in S_{TG}, p \in L \tag{81}$$

$$s_{sp} - \text{sS}_{s,\text{Sub},p} \geq 0, , \quad s \in S_{TG}, p \in L \tag{82}$$

$$s_{s,\text{High}} - s_{s,\text{Low}} \geq 0, \quad s \in S_{TG} \tag{83}$$

Isentropic turbine:

$$\mathrm{SS}_{s,\mathrm{OverS,High}} - \mathrm{SS}_{s,\mathrm{OverS,Low}} = 0, \quad s \in S_{TG} \tag{84}$$

Isentropic pump:

$$\mathrm{sS}_{s,\mathrm{SubS,High}} - \mathrm{sS}_{s,\mathrm{SubS,Low}} = 0, \quad s \in S_{TG} \tag{85}$$

Actual turbine enthalpy change:

$$\eta_T \left(\mathrm{HS}_{s,\mathrm{OverS,High}} - \mathrm{HS}_{s,\mathrm{OverS,Low}}\right) - \left(\mathrm{HS}_{s,\mathrm{Over,High}} - \mathrm{HS}_{s,\mathrm{Over,Low}}\right) = 0, \quad s \in S_{TG} \tag{86}$$

Actual pump enthalpy change:

$$\eta_P \left(\mathrm{hS}_{s,\mathrm{Sub,High}} - \mathrm{hS}_{s,\mathrm{Sub,Low}}\right) - \left(\mathrm{hS}_{s,\mathrm{SubS,High}} - \mathrm{hS}_{s,\mathrm{SubS,Low}}\right) = 0, \quad s \in S_{TG} \tag{87}$$

Where η_T, η_P are the isentropic efficiencies. Remaining enthalpies:

$$\mathrm{hS}_{s,\mathrm{Sub,Low}} - \mathrm{hS}_{s,\mathrm{SubS,Low}} = 0, \quad s \in S_{TG} \tag{88}$$

$$\mathrm{HS}_{s,\mathrm{Over,High}} - \mathrm{HS}_{s,\mathrm{OverS,High}} = 0, \quad s \in S_{TG} \tag{89}$$

Molar Heat transfered:

$$Q_{sp} = \mathrm{HS}_{s,\mathrm{OverS},p} - \mathrm{hS}_{s,\mathrm{SubS},p} \tag{90}$$

Pump and turbine work (positive form):

$$\left(W_P\right)_s = \left(\mathrm{hS}_{s,\mathrm{Sub,High}} - \mathrm{hS}_{s,\mathrm{Sub,Low}}\right) \tag{91}$$

$$\left(W_T\right)_s = \left(\mathrm{HS}_{s,\mathrm{Over,High}} - \mathrm{HS}_{s,\mathrm{Over,Low}}\right) \tag{92}$$

(5) Single stage $\overline{\boldsymbol{U}}_s^1\left(\overline{\boldsymbol{P}}_s, \overline{\boldsymbol{T}}_s, \overline{\boldsymbol{z}}_s, \overline{\boldsymbol{X}}\right) \leq 0$

In general, the heat source and sink have two fixed temperatures at which they enter and leave the heat exchangers. The mole flow of the heat source (nW) is also fixed and all these variables must be known beforehand. The minimum temperature approach is enforced not only at the inlet and outlet, but also for the internal two-phase points. The following equations represent these goals. For the heat source inlet (Twmn) and outlet (Twmx) temperatures:

$$\mathrm{TS}_{1,\mathrm{Sub,High}} + 5 \leq \mathrm{Twmn} \tag{93}$$

$$\mathrm{TS}_{1,\mathrm{Over,High}} + 5 \leq \mathrm{Twmx} \tag{94}$$

Note that the index s: $s = 1$. Internal two-phase points of the cycle with the heat source temperature matches ($\mathrm{TwH}_{s\pi}$):

$$T_{1,\pi,\mathrm{High}} + 5 \leq \mathrm{TwH}_{1,\pi}, \quad \pi \in \Pi \tag{95}$$

and their respective counterparts with the heat sink (with TwCmin for inlet and TwCmax for outlet):

$$\mathrm{TS}_{s,\mathrm{Sub,Low}} - 5 \geq \mathrm{TwCmn}, \quad s \in S_{TG} \tag{96}$$

$$\mathrm{TS}_{s,\mathrm{Over,Low}} - 5 \geq \mathrm{TwCmx}, \quad s \in S_{TG} \tag{97}$$

$$T_{s\pi,\mathrm{Low}} - 5 \geq \mathrm{TwC}_{s\pi}, \quad s \in S_{TG}, \pi \in \Pi \tag{98}$$

Note that the s index was intentionally left open, but for a single stage is strictly equal to 1.

The heat balances are defined for both heat source and sink:

$$\mathrm{nH} \cdot \mathrm{DHHT} = n_1 Q_{1,\mathrm{High}} \tag{99}$$

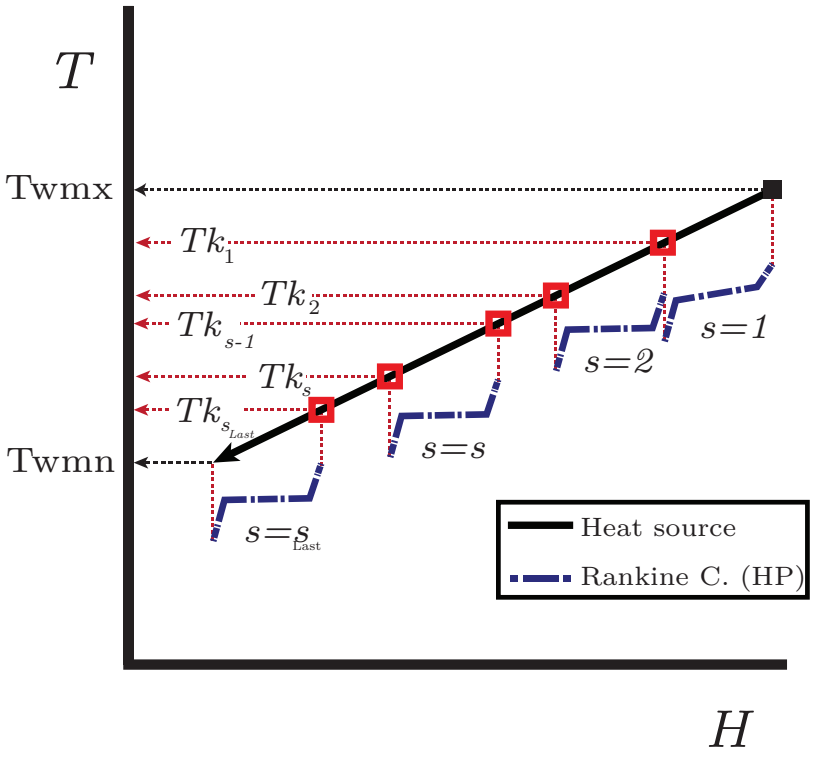

Figure 8: Temperature matches.

$$\mathrm{nC}_s \cdot 75.3120 \left(\mathrm{TwCmx} - \mathrm{TwCmn}\right) = n_s Q_{s,\mathrm{Low}},, \quad s \in S_{TG} \tag{100}$$

and the internal two phase points of the cycle as well:

$$n_1 \left(\mathrm{Hp}_{1,\pi,\mathrm{High}} - \mathrm{hS}_{1,\mathrm{Sub,High}}\right) = \mathrm{nH} \cdot \mathrm{dHHS}_{1,\pi}, \quad \pi \in \Pi \tag{101}$$

$$n_s \left(\mathrm{Hp}_{s,\pi,\mathrm{Low}} - \mathrm{hS}_{s,\mathrm{Sub,Low}}\right) = \mathrm{nC}_s \cdot 75.3119 \left(\mathrm{TwC}_{s\pi} - \mathrm{TwCmn}\right), \quad s \in S_{TG}, \pi \in \Pi \tag{102}$$

Finally, the constraints representing the enthalpy point at the two phase regions of the cycle ($\mathrm{Hp}_{s\pi p}$) and the enthalpy change of the heat source at the temperature matches are:

$$\mathrm{Hp}_{s\pi p} = h_{sp} + \psi_\pi \left(H_{sp} - h_{sp}\right) \tag{103}$$

$$\mathrm{Hu}\left(\mathrm{dHHS}_{s\pi}\right)=\frac{\mathrm{cplW1}}{3}\left[\left(\mathrm{TwH}_{s\pi}\right)^{3}-\mathrm{Twmn}^{3}\right]+\frac{\mathrm{cplW2}}{2}\left[\left(\mathrm{TwH}_{s\pi}\right)^{2}-\mathrm{Twmn}^{2}\right]+\mathrm{cplW3}\left[\mathrm{TwH}_{s\pi}-\mathrm{Twmn}\right] \tag{104}$$

(6) Multi-Stage Cascade $\overline{\boldsymbol{U}}_{s}^{C}\left(\overline{\boldsymbol{P}}_{s},\overline{\boldsymbol{T}}_{s},\overline{\boldsymbol{z}}_{s},\overline{\boldsymbol{X}}\right)\leq 0$

The Cascade configuration involves the successive heat transfer from the heat source to the first cycle, from the first cycle to second one and so on, until the last cycle is reached which then rejects the remaining heat to the sink. Modeling the temperature and enthalpy $T-H$ changes in the heat exchangers between cycles is considerably more difficult than the usual single-phase heat sink and source exchangers. In the in-between cycle exchangers, there are two liquid, vapor and two-phase regions and none of the $T-H$ models are the same for these regions. In addition, a minimum temperature approach must be enforced so heat transfer can take place (i.e. a minimum temperature approach must be enforced over the whole enthalpy change). This means that at the solution process the solver would have to *switch* from different $T-H$ equations depending on which phase the minimum temperature approaches are active. One way of solving these issues would be implementing disjunctions over the $T-H$ equations and defining a number of enthalpy points for the minimum temperature to be checked. The application of disjunctions is performed through generalized disjunctive programming (GDP) [24]. The GDP model in this case includes a new decision: the phase at which each of these temperature approach occur.

As shown in Figure 9, the selected enthalpy points to be matched were the low pressure dew point (LPDP) and the high pressure bubble point (HPBP). The selection of these two points simplifies the whole scheme because it is highly unlikely that each of these two points would cross more than two regions, i.e. the LPDP match will not occur before the bubble point of the next cycle at high pressure and neither the HPBP match beyond the dew point of the previous cycle.

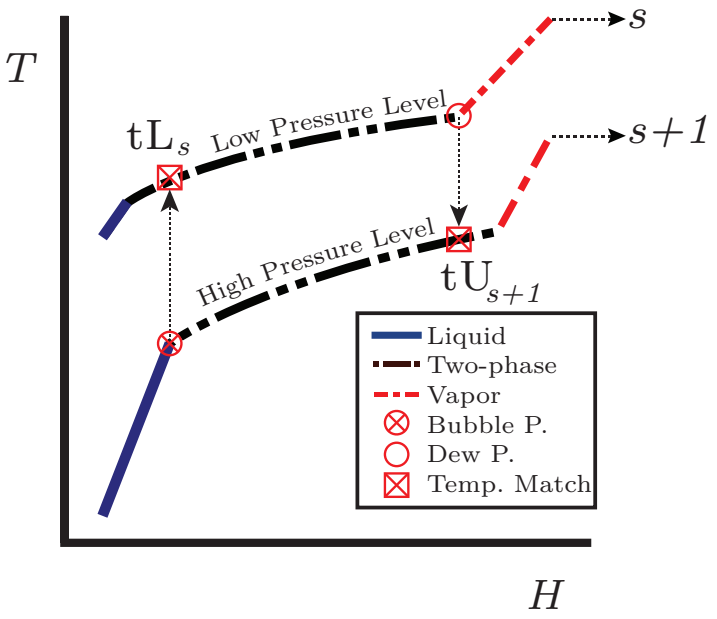

Figure 9: Cycle profiles inside the heat exchanger and the selected enthalpy points. Note that this is a case where both temperature matches lie on the two phase region, but it is not restricted to that case.

We now define the equations that are required only for the cascade multistage configuration. First, all of the equations of the single stage heat source and sink matches also apply here, with only one modification: $s = S_L$ in equations (96) through (98), (100), (102) and (103). Furthermore, the appropriate heat balances in between cycles and the minimum temperature approach constraints are defined.

Inter-stage heat balance:

$$n_s Q_{s,\text{Low}} = n_{s+1} Q_{s+1,\text{High}}, \quad s|s < S_L \tag{105}$$

Minimum temperature approach at the low pressure region (temperature match approximations with temperatures defined in Figure 9):

$$\text{tL}_s - 5 \geq T_{s+1,\text{Bubl,High}}, \quad s|s < S_L \tag{106}$$

Minimum temperature approach at the high pressure region:

$$\mathrm{tU}_{s+1} + 5 \leq T_{s,\mathrm{Dew,Low}}, \quad s|s < S_L \tag{107}$$

Finally, only the disjunctive terms that allow to chose which enthalpy model is used to calculate the matching temperatures inside the heat exchangers are left to be defined. A disjunction will involve the enthalpy model for a single phase or a 2-phases; this is done once per enthalpy point for every heat exchanger that is located in between cycles (or $s-1$ heat exchangers). The logic dictates that only one of the two phases available for each point must be selected. All these statements are included in the following equations:

$$\begin{pmatrix} \hat{Y}_s^{\mathrm{liq}} \\ \bar{t}_s^L\,(\mathrm{liq}) = 0 \end{pmatrix} \vee \begin{pmatrix} \hat{Y}_s^{\mathrm{2P}} \\ \bar{t}_s^L\,(\mathrm{2P}) = 0 \end{pmatrix} \tag{108}$$
$$\hat{Y}_s^{\mathrm{liq}} \underline{\vee} \hat{Y}_s^{\mathrm{2P}}$$

$$\begin{pmatrix} \check{Y}_s^{\mathrm{vap}} \\ \bar{t}_s^U\,(\mathrm{vap}) = 0 \end{pmatrix} \vee \begin{pmatrix} \check{Y}_s^{\mathrm{2P}} \\ \bar{t}_s^U\,(\mathrm{2P}) = 0 \end{pmatrix} \tag{109}$$
$$\check{Y}_s^{\mathrm{vap}} \underline{\vee} \check{Y}_s^{\mathrm{2P}}$$

where the Y_s are boolean variables, and the $\bar{t}$ are the respective set of constraints for phase match. The last remark on the implementation of these constraints, is that GDP models can be reformulated into MINLP models by using the big-M (BM) of Hull-Reformulation (HR) [25]. The Big-M reformulation was chosen since its easier to implement. The following subsections will display the equations that go inside each disjunctive term.

(a) Disjunction 1: Low pressure; Term 1:Liquid match $\bar{t}_s^L\,(\mathbf{liq}) = 0$

If the match is between the liquid phase of the previous cycle, then the enthalpy model is:

$$
\begin{aligned}
&n_{s+1}\left[h_{s+1,\text{High}}-\text{hS}_{s+1,\text{Sub,High}}\right]= \\
&\frac{n_s}{\text{Hu}}\cdot \\
&\left[\frac{\text{cpx1}_i}{3}\left[\left(\text{tL}_s\right)^3-\left(\text{TS}_{s,\text{Sub,Low}}\right)^3\right]+\frac{\text{cpx2}_i}{2}\left[\left(\text{tL}_s\right)^2-\left(\text{TS}_{s,\text{Sub,Low}}\right)^2\right]+\text{cpx3}_i\left[\text{tL}_s-\left(\text{TS}_{s,\text{Sub,Low}}\right)\right]\right] \\
&\quad s|s<S_L
\end{aligned}
\tag{110}
$$

the heat balance must be consistent with the liquid phase:

$$
n_{s+1}\left[h_{s+1,\text{High}}-\text{hS}_{s+1,\text{Sub,High}}\right]<n_s\left[h_{s,\text{Low}}-\text{hS}_{s,\text{Sub,Low}}\right],\quad s|s<S_L \tag{111}
$$

(b) Disjunction 1: Low pressure; Term 2:Two-Phase match $\bar{t}_s^L\left(\mathbf{2P}\right)=0$

If the match is between the two phase region of the previous cycle, then the enthalpy model is then *approximated* by the following constraints:

$$
n_{s+1}\left[h_{s+1,\text{High}}-\text{hS}_{s+1,\text{Sub,High}}\right]=n_s\left[h_{s,\text{Low}}+\text{VL}_s\left(H_{s,\text{Low}}-h_{s,\text{Low}}\right)-\text{hS}_{s,\text{Sub,Low}}\right],\quad s|s<S_L \tag{112}
$$

where VL_s stands for the vapor fraction of the approximation. Then, the temperature is approximated using the following equation:

$$
\text{tL}_s-T_{s,\text{Bubl,Low}}=\text{VL}_s\left(T_{s,\text{Dew,Low}}-T_{s,\text{Bubl,Low}}\right),\quad s\in S_{TG} \tag{113}
$$

Finally, if the temperature tL_s is at the two phase region, the heat balance must be consistent (and the equality must be in opposite direction with reference to eq. (111)):

$$
n_{s+1}\left[h_{s+1,\text{High}}-\text{hS}_{s+1,\text{Sub,High}}\right]>n_s\left[h_{s,\text{Low}}-\text{hS}_{s,\text{Sub,Low}}\right],\quad s|s<S_L \tag{114}
$$

(c) Disjunction 2: High pressure; Term 1:Two-Phase match $\bar{t}_s^U\,(\mathbf{2P}) = 0$

If the match is between the two phase region of the previous cycle, then the enthalpy model is:

$$n_s\left[h_{s,\text{Low}} - \text{hS}_{s,\text{Sub,Low}}\right] = n_{s+1}\left[h_{s+1,\text{High}} + \psi_u\left(H_{s+1,\text{High}} - h_{s+1,\text{High}}\right) - \text{hS}_{s+1,\text{Sub,High}}\right], \quad s|s < S_L \tag{115}$$

$$\text{tU}_s - T_{s,\text{Bubl,High}} = \psi_u\left(T_{s,\text{Dew,High}} - T_{s,\text{Bubl,High}}\right), \quad s \in S_{TG} \tag{116}$$

and the corresponding heat balance constraint for the two-phases region:

$$n_s\left[\text{HS}_{s,\text{Over,Low}} - H_{s,\text{Low}}\right] > n_{s+1}\left[\text{HS}_{s+1,\text{Over,High}} - H_{s+1,\text{High}}\right], \quad s|s < S_L \tag{117}$$

(d) Disjunction 2: High pressure; Term 2:Vapor match $\bar{t}_s^U\,(\mathbf{vap}) = 0$

The match over the vapor region includes all individual variables of the EOS with the $G_{s\pi fp}$=1 simplification (i.e. no activity coefficients model calculation):

$$\text{fTu}_{is} = \left[1 + c_{\omega,i}\left(1 - \left(\text{tU}_s/\text{Tc}_i\right)^{0.5}\right)\right]^2 \tag{118}$$

$$\text{au}_{is} = \frac{0.42748 R_g \text{Tc}_i^2\left(\text{fTu}\right)_{is}}{\text{Pc}_i b_i\left(\text{tU}_s\right)} \tag{119}$$

$$\text{bu}_s = \frac{\hat{b}_{s,\text{Dew,High}} P_{s,\text{High}}}{R_g\left(\text{tU}_s\right)} \tag{120}$$

$$\hat{\text{au}}_s = -\frac{1}{0.64663}\left(\sum_{i\in I} z_{is} \ln \frac{\hat{b}_{s,\text{Dew,High}}}{b_i}\right) + \sum_{i\in I} z_{is}\left(\text{au}_{is}\right) \tag{121}$$

$$(\mathrm{Zu}_s)^3 - (\mathrm{Zu}_s)^2 + \left[-\mathrm{bu}_s - (\mathrm{bu}_s)^2 + \hat{\mathrm{au}}_s \mathrm{bu}_s\right] \mathrm{Zu}_s - \hat{\mathrm{au}}_s (\mathrm{bu}_s)^2 = 0, \quad s \in S_{TG} \tag{122}$$

$$3 (\mathrm{Zu}_s)^2 - 2 (\mathrm{Zu}_s) + \left[-\mathrm{bu}_s - (\mathrm{bu}_s)^2 + \hat{\mathrm{au}}_s \mathrm{bu}_s\right] \geq 0, \quad s \in S_{TG} \tag{123}$$

$$6 (\mathrm{Zu}_s) - 2 \geq 0, \quad s \in S_{TG} \tag{124}$$

$$\mathrm{fTup}_{is} = -\frac{c_{\omega,i}}{\mathrm{Tc}_i} \left[1 + c_{\omega,i} \left(1 - (\mathrm{tU}_s/\mathrm{Tc}_i)^{0.5}\right)\right] \left(\frac{\mathrm{tU}_s}{\mathrm{Tc}_i}\right)^{-0.5} \tag{125}$$

$$\mathrm{aup}_{is} = 0.42748 (\mathrm{fTup}_{is}) \tag{126}$$

$$\hat{aup}_s = \left(\sum_{i \in I} z_{is} \frac{\mathrm{aup}_{is}}{b_i} \frac{R_g^2 \mathrm{Tc}_i^2}{\mathrm{Pc}_i}\right) + \frac{R_g}{\mathrm{A1}} \sum_{i \in I} z_{is} \ln \left(\frac{\hat{b}_{s,\mathrm{Dew,High}}}{b_i}\right) \tag{127}$$

$$\mathrm{HRu}_s = -\left(\hat{\mathrm{au}}_s - \frac{\hat{aup}_s}{R_g}\right) \ln \frac{\mathrm{Zu}_s}{\mathrm{Zu}_s + \mathrm{bu}_s} + 1 - \mathrm{Zu}_s \tag{128}$$

$$\mathrm{Hu}\left(\mathrm{DHiu}_{is}\right) = \frac{\mathrm{cpx1}_i}{3} \left[(\mathrm{tU}_s)^3 - 298.15^3\right] + \frac{\mathrm{cpx2}_i}{2} \left[(\mathrm{tU}_s)^2 - 298.15^2\right] + \mathrm{cpx3}_i \left[\mathrm{tU}_s - 298.15\right] \tag{129}$$

$$\mathrm{Hup}_{sp} = \sum_{i \in I} z_{is} \left[\frac{\mathrm{DHF}_i}{\mathrm{Hu}} + (\mathrm{DHiu}_{is})\right] - \mathrm{HRu}_s \mathrm{tU}_s \frac{8.314}{\mathrm{Hu}} \tag{130}$$

Heat balance:

$$n_s \left(H_{s,\text{Low}} - \text{hS}_{s,\text{Sub,Low}}\right) = n_{s+1} \left(\text{Hup}_{s+1,p} - \text{hS}_{s+1,\text{Sub,High}}\right), \quad s|s < S_L \tag{131}$$

and heat consistency:

$$n_s \left[\text{HS}_{s,\text{Over,Low}} - H_{s,\text{Low}}\right] < n_{s+1} \left[\text{HS}_{s+1,\text{Over,High}} - H_{s+1,\text{High}}\right], \quad s|s < S_L \tag{132}$$

(7) Multi-Stage Series $\overline{\boldsymbol{U}}_s^S \left(\overline{\boldsymbol{P}}_s, \overline{\boldsymbol{T}}_s, \overline{\boldsymbol{z}}_s, \overline{\boldsymbol{X}}\right) \leq 0$

The series cascade configuration is rather simple in comparison to the single cascade configuration, since all the cycles absorb and reject heat to a single-phase source or sink. The series cascade configuration requires a partition of the heat source $T-H$ profile which will lead to a series of heat balances and minimum temperature approach equations. The heat source will be partitioned in $s-1$ internal temperatures Tk_s (note that $s > 1$) as shown in Figure 10.

The corresponding heat balance of the partitions reads:

$$n_s Q_{s,\text{High}} = \text{nH} \cdot \Delta\text{He}_s, \quad s \in S_{TG} \tag{133}$$

where ΔHe_s is the overall enthalpy change of the partition which for the equally spaced profile is given by DHHT divided by the total number of stages. Each one of these internal partitions will have its own temperature matches in the two-phase region of each cycle. For this, equation (103) must be augmented using the following balances:

$$n_s \left(\text{Hp}_{s,\pi,\text{High}} - \text{hS}_{s,\text{Sub,High}}\right) = \text{nH} \cdot \text{dHHX}_{s,\pi}, \quad s \in S_{TG}, \pi \in \Pi \tag{134}$$

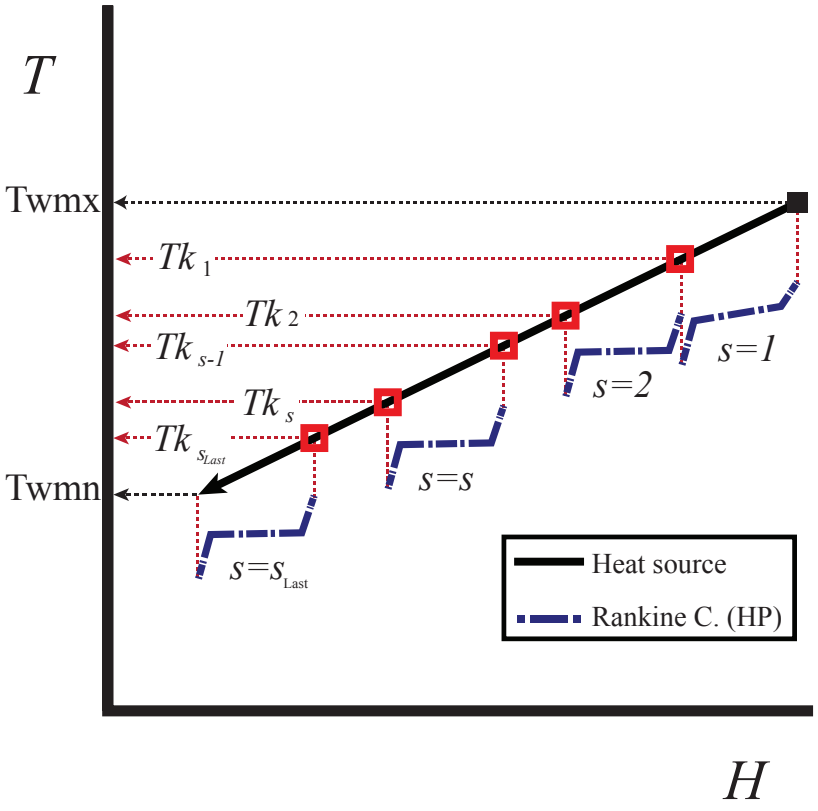

Figure 10: Multi-Stage series RC, generalization at high pressure level of the cycle.

$$\mathrm{Hu}\left(\mathrm{dHHX}_{s\pi}\right) = \frac{\mathrm{cplW1}}{3}\left[\left(\mathrm{TwH}_{s\pi}\right)^3 - \mathrm{Tk}_s^3\right] + \frac{\mathrm{cplW2}}{2}\left[\left(\mathrm{TwH}_{s\pi}\right)^2 - \mathrm{Tk}_s^2\right] + \mathrm{cplW3}\left[\mathrm{TwH}_{s\pi} - \mathrm{Tk}_s\right] \tag{135}$$

$$\mathrm{Hu}\left(\mathrm{dHHX}_{\mathrm{Last},\pi}\right) = \frac{\mathrm{cplW1}}{3}\left[\left(\mathrm{TwH}_{\mathrm{Last},\pi}\right)^3 - \mathrm{Twmn}^3\right] + \frac{\mathrm{cplW2}}{2}\left[\left(\mathrm{TwH}_{\mathrm{Last},\pi}\right)^2 - \mathrm{Twmn}^2\right] + \mathrm{cplW3}\left[\mathrm{TwH}_{\mathrm{Last},\pi} - \mathrm{Twmn}\right] \tag{136}$$

The corresponding constraints of the minimum temperature matches are the following:

$$\mathrm{TS}_{s,\mathrm{Sub,High}} + 5 \leq \mathrm{Tk}_s \quad s|s < S_L \tag{137}$$

$$\mathrm{TS}_{s+1,\mathrm{Over,High}} + 5 \leq \mathrm{Tk}_s \quad s|s < S_L \tag{138}$$

$$\mathrm{TS}_{S_L,\mathrm{Sub,High}} + 5 \leq \mathrm{Twmn} \tag{139}$$

$$\mathrm{TS}_{1,\mathrm{Over,High}} + 5 \leq \mathrm{Twmx} \tag{140}$$

Two-phase points.

$$T_{s\pi,\mathrm{High}} + 5 \leq \mathrm{TwH}_{s\pi}, \quad s \in S_{TG}, \pi \in \Pi \tag{141}$$

Finally, all the balances and constraints involving the temperature at the heat sink and low-pressure region of the cycle are the same as in the case of a single stage (i.e. equations (96) through (98), (100) and (102)).

(8) Efficiency

The efficiency for the cascade configuration (and single stage as well) is calculated as follows:

$$(\eta_I) = \frac{\sum_{s\in S_{TG}} n_s \left(W_T\right)_s - \sum_{s\in S_{TG}} n_s \left(W_P\right)_s}{n_1 Q_{1,\text{High}}} \tag{142}$$

whereas for the the series cascade configuration reads:

$$(\eta_I) = \frac{\sum_{s\in S_{TG}} n_s \left(W_T\right)_s - \sum_{s\in S_{TG}} n_s \left(W_P\right)_s}{\sum_{s\in S_{TG}} n_s Q_{s,\text{High}}} \tag{143}$$

(9) Sizing and Costing $\overline{\boldsymbol{C}}_s \left(\overline{\boldsymbol{P}}_s, \overline{\boldsymbol{T}}_s, \overline{\boldsymbol{z}}_s, \overline{\boldsymbol{X}}\right) = 0$

The processing cost of the basic modules of the RC was implemented for its inclusion as part of the objective function. The modules of the RC are: heat exchanger, turbines and pumps.

The sizing of the heat exchangers depends on the physical configuration, materials of construction, the overall heat transfer coefficients, temperatures and heat balances. In this work we adopted a basic approach by fixing the first three terms, and considering the temperature and heat variables as decision variables. Evidently those assumptions will result in a kind of shortcut design. However, the results will provide an estimation of the cost contribution of the heat exchangers.

Tube and shell heat exchangers were selected with split-ring head construction (TEMA S) using 3/4 in outside diameter × 14 BWG low carbon steel tubes on a 15/16 equilateral triangular pitch, and one tube-side pass [26]. It should be noted that no pressure drop along the exchangers and constant overall heat transfer coefficients were assumed. The aim of the first assumption is to avoid modeling the pressure profile along the heat exchanger which in turn removes the deployment of differential equations to model such a profile. Overall heat transfer coefficient were estimated from typical values of film coefficients.

The equations for the sizing of the heat exchangers are the logarithmic mean tem-

perature differences (LMTD) and areas. Considering that there is more than one stage configuration, the single stage equations will be presented first. The LMTD equations are defined for three sections of each exchanger, namely liquid phase, two-phases and vapor phase (indexes l', e' and v'), and two pressure sides, high and low (superscripts H and L):

$$\left(\mathrm{LMTD}^{H}_{l'}\right)_s = \left[\left(\mathrm{TwH}_{s,\mathrm{Bubl}} - T_{s,\mathrm{Bubl,High}}\right) - \left(\mathrm{Twmn} - \mathrm{TS}_{s,\mathrm{Sub,High}}\right)\right] / \ln\left(\frac{\mathrm{TwH}_{s,\mathrm{Bubl}} - T_{s,\mathrm{Bubl,High}}}{\mathrm{Twmn} - \mathrm{TS}_{s,\mathrm{Sub,High}}}\right) \tag{144}$$

$$\left(\mathrm{LMTD}^{H}_{e'}\right)_s = \left[\left(\mathrm{TwH}_{s,\mathrm{Dew}} - T_{s,\mathrm{Dew,High}}\right) - \left(\mathrm{TwH}_{s,\mathrm{Bubl}} - T_{s,\mathrm{Bubl,High}}\right)\right] / \ln\left(\frac{\mathrm{TwH}_{s,\mathrm{Dew}} - T_{s,\mathrm{Dew,High}}}{\mathrm{TwH}_{s,\mathrm{Bubl}} - T_{s,\mathrm{Bubl,High}}}\right) \tag{145}$$

$$\left(\mathrm{LMTD}^{H}_{v'}\right)_s = \left[\left(\mathrm{Twmx} - \mathrm{TS}_{s,\mathrm{Over,High}}\right) - \left(\mathrm{TwH}_{s,\mathrm{Dew}} - T_{s,\mathrm{Dew,High}}\right)\right] / \ln\left(\frac{\mathrm{Twmx} - \mathrm{TS}_{s,\mathrm{Over,High}}}{\mathrm{TwH}_{s,\mathrm{Dew}} - T_{s,\mathrm{Dew,High}}}\right) \tag{146}$$

$$\left(\mathrm{LMTD}^{L}_{l'}\right)_s = \left[\left(T_{s,\mathrm{Bubl,Low}} - \mathrm{TwC}_{s,\mathrm{Bubl}}\right) - \left(\mathrm{TS}_{s,\mathrm{Sub,Low}} - \mathrm{TwCmn}\right)\right] / \ln\left(\frac{T_{s,\mathrm{Bubl,Low}} - \mathrm{TwC}_{s,\mathrm{Bubl}}}{\mathrm{TS}_{s,\mathrm{Sub,Low}} - \mathrm{TwCmn}}\right) \tag{147}$$

$$\left(\mathrm{LMTD}^{L}_{e'}\right)_s = \left[\left(T_{s,\mathrm{Dew,Low}} - \mathrm{TwC}_{s,\mathrm{Dew}}\right) - \left(T_{s,\mathrm{Bubl,Low}} - \mathrm{TwC}_{s,\mathrm{Bubl}}\right)\right] / \ln\left(\frac{T_{s,\mathrm{Dew,Low}} - \mathrm{TwC}_{s,\mathrm{Dew}}}{T_{s,\mathrm{Bubl,Low}} - \mathrm{TwC}_{s,\mathrm{Bubl}}}\right) \tag{148}$$

$$\left(\mathrm{LMTD}^{L}_{v'}\right)_s = \left[\left(\mathrm{TS}_{s,\mathrm{Over,Low}} - \mathrm{TwCmx}\right) - \left(T_{s,\mathrm{Dew,Low}} - \mathrm{TwC}_{s,\mathrm{Dew}}\right)\right] / \ln\left(\frac{\mathrm{TS}_{s,\mathrm{Over,Low}} - \mathrm{TwCmx}}{T_{s,\mathrm{Dew,Low}} - \mathrm{TwC}_{s,\mathrm{Dew}}}\right) \tag{149}$$

The area equations are defined for the same sections of the heat exchangers of the LMTDs.

$$A^{H}_{l'} = \frac{\mathrm{nH} \cdot \mathrm{dHHS}_{1,\mathrm{Bubl}} \cdot \mathrm{Hu} \cdot 1000}{\left(\mathrm{LMTD}^{H}_{l'}\right)_1 \cdot U_{l'}} \tag{150}$$

$$A^{H}_{e'} = \frac{\mathrm{nH} \cdot \left(\mathrm{dHHS}_{1,\mathrm{Dew}} - \mathrm{dHHS}_{1,\mathrm{Bubl}}\right) \cdot \mathrm{Hu} \cdot 1000}{\left(\mathrm{LMTD}^{H}_{e'}\right)_1 \cdot U_{e'}} \tag{151}$$

$$A^{H}_{v'} = \frac{\mathrm{nH} \cdot \left(\mathrm{DHHT} - \mathrm{dHHS}_{1,\mathrm{Dew}}\right) \cdot \mathrm{Hu} \cdot 1000}{\left(\mathrm{LMTD}^{H}_{v'}\right)_1 \cdot U_{v'}} \tag{152}$$

$$\left(A^{L}_{l'}\right)_s = \frac{\mathrm{nC}_s \cdot 75.3119 \left(\mathrm{TwC}_{s,\mathrm{Bubl}} - \mathrm{TwCmn}\right)}{\left(\mathrm{LMTD}^{L}_{l'}\right)_s \cdot U_{l'}} \tag{153}$$

$$\left(A^L_{e'}\right)_s = \frac{\mathrm{nC}_s \cdot 75.3119\,(\mathrm{TwC}_{s,\mathrm{Dew}} - \mathrm{TwC}_{s,\mathrm{Bubl}})}{\left(\mathrm{LMTD}^L_{e'}\right)_s \cdot U_{e'}} \tag{154}$$

$$\left(A^L_{v'}\right)_s = \frac{\mathrm{nC}_s \cdot 75.3119\,(\mathrm{TwCmx} - \mathrm{TwC}_{s,\mathrm{Dew}})}{\left(\mathrm{LMTD}^L_{v'}\right)_s \cdot U_{v'}} \tag{155}$$

Where the parameters U are the overall heat transfer coefficients taken from [26] and [27] tables. Then the updated bare cost of the heat exchangers is given by the summation of the areas of the three sections for each exchanger and some coefficients for the updated cost [28]:

$$B^H_{CX} = F_{0X} \cdot \left(\frac{A^H_{l'} + A^H_{e'} + A^H_{v'}}{S_{0X}}\right)^{\alpha_X} \tag{156}$$

$$\left(B^L_{CX}\right)_s = F_{0X} \cdot \left(\frac{\left(A^L_{l'}\right)_s + \left(A^L_{e'}\right)_s + \left(A^L_{v'}\right)_s}{S_{0X}}\right)^{\alpha_X} \tag{157}$$

where the F_{0X} parameter takes into account the material, pressure and adjust for inflation factors (or C0·UF·BC(MPF+MF-1) in terms of [28] notation, which they were taken from). For the cascade multi-stage configuration heat transfer in between cycles in the intermediate heat exchanger takes place. So, all these exchangers must be sized with the same kind of equations that were used previously (with the change of $s = S_L$ for exchanger of the heat sink) and the additional LMTDs and areas for the intermediate exchangers:

$$\left(\mathrm{LMTD}^i_{l'}\right)_s = \\ \left[(T_{s-1,\mathrm{Bubl,Low}} - T_{s,\mathrm{Bubl,High}}) - (\mathrm{TS}_{s-1,\mathrm{Sub,Low}} - \mathrm{TS}_{s,\mathrm{Sub,High}})\right] / \ln\left(\frac{T_{s-1,\mathrm{Bubl,Low}} - T_{s,\mathrm{Bubl,High}}}{\mathrm{TS}_{s-1,\mathrm{Sub,Low}} - \mathrm{TS}_{s,\mathrm{Sub,High}}}\right), \\ s|s > 1 \tag{158}$$

$$\left(\mathrm{LMTD}^{i}_{e'}\right)_s =$$

$$\left[\left(T_{s-1,\mathrm{Dew,Low}} - T_{s,\mathrm{Dew,High}}\right) - \left(T_{s-1,\mathrm{Bubl,Low}} - T_{s,\mathrm{Bubl,High}}\right)\right] / \ln\left(\frac{T_{s-1,\mathrm{Dew,Low}} - T_{s,\mathrm{Dew,High}}}{T_{s-1,\mathrm{Bubl,Low}} - T_{s,\mathrm{Bubl,High}}}\right),$$

$$s|s > 1 \tag{159}$$

$$\left(\mathrm{LMTD}^{i}_{v'}\right)_s =$$

$$\left[\left(\mathrm{TS}_{s-1,\mathrm{Over,Low}} - \mathrm{TS}_{s,\mathrm{Over,High}}\right) - \left(T_{s-1,\mathrm{Dew,Low}} - T_{s,\mathrm{Dew,High}}\right)\right] / \ln\left(\frac{\mathrm{TS}_{s-1,\mathrm{Over,Low}} - \mathrm{TS}_{s,\mathrm{Over,High}}}{T_{s-1,\mathrm{Dew,Low}} - T_{s,\mathrm{Dew,High}}}\right),$$

$$s|s > 1 \tag{160}$$

$$\left(A^{i}_{l'}\right)_s = \frac{n_s \cdot \left(h_{s,\mathrm{High}} - \mathrm{hS}_{s,\mathrm{Sub,High}}\right) \cdot \mathrm{Hu} \cdot 1000}{\left(\mathrm{LMTD}^{i}_{l'}\right)_s \cdot U^{i}_{l'}} \tag{161}$$

$$\left(A^{i}_{e'}\right)_s = \mathrm{Hu} \cdot 1000 \cdot$$

$$\frac{\left[n_{s-1}\left(\mathrm{HS}_{s-1,\mathrm{Over,Low}} - \mathrm{hS}_{s-1,\mathrm{Sub,Low}}\right) - n_s\left(h_{s,\mathrm{High}} - \mathrm{hS}_{s,\mathrm{Sub,High}}\right) - n_{s-1}\left(\mathrm{HS}_{s-1,\mathrm{Over,Low}} - H_{s-1,\mathrm{Low}}\right)\right]}{\left(\mathrm{LMTD}^{i}_{e'}\right)_s \cdot U^{i}_{e'}},$$

$$s|s > 1 \tag{162}$$

$$\left(A^{i}_{v'}\right)_s = \frac{n_{s-1} \cdot \left(\mathrm{HS}_{s-1,\mathrm{Over,Low}} - H_{s-1,\mathrm{Low}}\right) \cdot \mathrm{Hu} \cdot 1000}{\left(\mathrm{LMTD}^{i}_{v'}\right)_s \cdot U^{i}_{v'}}, \quad s|s > 1 \tag{163}$$

$$\left(B^{i}_{CX}\right)_s = F_{0X} \cdot \left(\frac{\left(A^{i}_{l'}\right)_s + \left(A^{i}_{e'}\right)_s + \left(A^{i}_{v'}\right)_s}{S_{0X}}\right)^{\alpha_X} \tag{164}$$

The series cascade model requires equation (150) for the stage $s = S_L$, (151) for all s, (152) for $s = 1$, (153) to (155) and their respective areas given by equations (153)-(155). Also the following equations for the rest of the stages:

$$\left(\mathrm{LMTD}^{H}_{l'}\right)_s = \left[\left(\mathrm{TwH}_{s,\mathrm{Bubl}} - T_{s,\mathrm{Bubl,High}}\right) - \left(\mathrm{Tk}_s - \mathrm{TS}_{s,\mathrm{Sub,High}}\right)\right] / \ln\left(\frac{\mathrm{TwH}_{s,\mathrm{Bubl}} - T_{s,\mathrm{Bubl,High}}}{\mathrm{Tk}_s - \mathrm{TS}_{s,\mathrm{Sub,High}}}\right) \tag{165}$$

$$\left(\mathrm{LMTD}^{H}_{v'}\right)_s = \left[\left(\mathrm{Tk}_{s-1} - \mathrm{TS}_{s,\mathrm{Over,High}}\right) - \left(\mathrm{TwH}_{s,\mathrm{Dew}} - T_{s,\mathrm{Dew,High}}\right)\right] / \ln\left(\frac{\mathrm{Tk}_{s-1} - \mathrm{TS}_{s,\mathrm{Over,High}}}{\mathrm{TwH}_{s,\mathrm{Dew}} - T_{s,\mathrm{Dew,High}}}\right) \tag{166}$$

$$\left(A^{H}_{l'}\right)_s = \frac{\mathrm{nH} \cdot \mathrm{dHHX}_{s,\mathrm{Bubl}} \cdot \mathrm{Hu} \cdot 1000}{\left(\mathrm{LMTD}^{H}_{l'}\right)_s \cdot U_{l'}} \tag{167}$$

$$\left(A^{H}_{e'}\right)_s = \frac{\mathrm{nH}\left(\mathrm{dHHX}_{s,\mathrm{Dew}} - \mathrm{dHHX}_{s,\mathrm{Bubl}}\right) \cdot \mathrm{Hu} \cdot 1000}{\left(\mathrm{LMTD}^{H}_{e'}\right)_s \cdot U_{e'}} \tag{168}$$

$$\left(A^{H}_{v'}\right)_s = \frac{\mathrm{nH}\left(\Delta\mathrm{He}_s - \mathrm{dHHX}_{s,\mathrm{Dew}}\right) \cdot \mathrm{Hu} \cdot 1000}{\left(\mathrm{LMTD}^{H}_{v'}\right)_s \cdot U_{v'}} \tag{169}$$

$$\left(B^{H}_{CX}\right)_s = F_{0X} \cdot \left(\frac{\left(A^{H}_{l'}\right)_s + \left(A^{H}_{e'}\right)_s + \left(A^{H}_{v'}\right)_s}{S_{0X}}\right)^{\alpha_X} \tag{170}$$

For the pump and turbine, the costing is done on the basis of the work required and produced respectively, adjusted by the mechanical efficiency:

$$\left(S_P\right)_s = 2298.2964 \cdot n_s \cdot \frac{\left(W_P\right)_s}{\eta_{MP}} \cdot \mathrm{Hu} \tag{171}$$

$$\left(S_T\right)_s = 1.3410 \cdot n_s \cdot \frac{\left(W_T\right)_s}{\eta_{MT}} \cdot \mathrm{Hu} \tag{172}$$

$$\left(B_{CP}\right)_s = F_{0P}\left[\frac{\left(S_P\right)_s}{S_{0P}}\right]^{\alpha_P} \tag{173}$$

$$\left(B_{CT}\right)_s = F_{0T}\left[\frac{\left(S_T\right)_s}{S_{0T}}\right]^{\alpha_T} \tag{174}$$

All these equations account for the fixed costs of the equipment. There are other costs related to the utilities. We only considered the cost of water for the heat source and cooling water for the heat sink. Both of these costs are calculated with a variable cost over an annual basis, so a yearly cost increase is taken into account.

The cost of water for a particular year yr is calculated with the simple yearly adjustment of the parameter $\mathrm{CSF}_{yr} = \mathrm{CSF}_0\left(1 + \mathrm{ir}\right)^{yr}$, and the CEPCI which for all the calculations in this paper assumed the value of 579.8 for October 2014 [29]. The cost for

water are defined in [30]. For water used as heat source the cost is:

$$\mathrm{PWW}_{yr} = 579.8 \left[0.0001 + \left(3.3399 \times 10^{-5}\right) \mathrm{nH}^{-0.6}\right] + 0.003 \cdot \mathrm{CSF}_{yr} \tag{175}$$

The cost of cooling water for single stage and cascade reads:

$$\mathrm{PCW}_{yr} = 579.8 \left[0.0001 + (0.0017)\, \mathrm{nC}_{s_{Last}}^{-1}\right] + 0.003 \cdot \mathrm{CSF}_{yr} \tag{176}$$

For the series model:

$$\mathrm{PCW}_{yr} = 579.8 \left[0.0001 + (0.0017) \left(\sum_{s \in S_{TG}} \mathrm{nC}_s\right)^{-1}\right] + 0.003 \cdot \mathrm{CSF}_{yr} \tag{177}$$

The annual cost of regular water and cooling water is given by:

$$\mathrm{CWW}_{yr} = \left(5.6813 \times 10^5\right) \mathrm{PWW}_{yr} \cdot \mathrm{nH} \tag{178}$$

Cooling cost for the single cascade:

$$\mathrm{CCW}_{yr} = \left(5.6813 \times 10^5\right) \mathrm{PCW}_{yr} \cdot \mathrm{nC}_{s_{Last}} \tag{179}$$

and the series model:

$$\mathrm{CCW}_{yr} = \left(5.6813 \times 10^5\right) \mathrm{PCW}_{yr} \cdot \sum_{s \in S_{TG}} \mathrm{nC}_s \tag{180}$$

The cost in the objective function consists of three parts: the overall updated module cost which is a fixed cost, the overall cost of water which varies each year, and the profit due to annual electricity production.

The overall module cost is the summation of the module costs, where the term $\left(B_{CX}^{i}\right)_s$

is only defined for the cascade model (i.e. zero otherwise):

$$F_C = \sum_{s \in S} \left[\left(B_{CX}^{H}\right)_s + \left(B_{CX}^{i}\right)_s + \left(B_{CX}^{L}\right)_s + \left(B_{CP}\right)_s + \left(B_{CT}\right)_s \right] \tag{181}$$

The cost of water consists of the regular and cooling water annual cost summation. For this a period of 10 years ($yrL = 10$) is assumed:

$$V_C = \sum_{yr=1}^{yrL} \left(\mathrm{CCW}_{yr} + \mathrm{CWW}_{yr} \right) \tag{182}$$

The annual electricity produced [MWh] (with an assumed availability of 90 % in each year):

$$E_G = 0.9 \cdot 3.1536 \times 10^4 \cdot \mathrm{Hu} \cdot \sum_{s \in S_{TG}} n_s \left[\left(W_T\right)_s - \left(W_P\right)_s \right] \tag{183}$$

Finally, the yearly cost over the whole 10 years span is defined as follows:

$$\tilde{C} = \frac{1.35 F_C + V_C}{E_G} \tag{184}$$

where a 35 % factor to account for the operations and maintenance cost was used.

4 Results

4.1 Comparison at configurations

In this section the optimal operating parameters and the optimal mixture composition for a single stage RC (Figure 1), two series-connected RCs (Figure 2) and two cascade-connected (Figure 3) are obtained. In all three cases, we would like to recover as much as energy as possible from the low-temperature heat source as measured trough the maximization of the first law efficiency and the minimization of the annual cost per electricity

ratio.

In Table 1 some essential operating parameters are shown. These include the processing conditions for the heat source which was assumed is hot water at ambient pressure. It should be noted that the number of components does not impose any limitation on the actual model, but it impacts the number of variables required to solve the problem. Nevertheless, only five components were chosen for the sake of simplicity. The available components are listed in Table 2. In Table 3 the heat capacity parameters for the model are displayed. These were fitted from the data used in [8]. The models were implemented in GAMS [31]; the NLP models (single and series model) were solved using the CONOPT solver [32] and the disjunctive model (cascade) was solved with the solver for extended mathematical programming (EMP) [33] using the Big-M reformulation and then solved via the SBB solver. It is important to note the use of deterministic techniques for the solution process of this problem. In other words, for all the solutions found in this work, we are certain of at least of local optimality. This is in contrast to meta-heuristics or stochastic approaches, where there is no guarantee of optimality. An efficient initialization of the problem was important because local optimization techniques were used, and occasionally several local solutions were found. An equimolar mixture with ideal liquid phase (i.e. all activity coefficients equal to 1) and ideal gas phase turned out to be a reasonable way to initialize the model. Other initial points were required specifically for the multi-stage models, in these cases the solution of the single stage model was used as initial point for each stage of the multi-stage scenario.

Each one of the models was solved for the conditions previously described. The optimal solutions are displayed in Table 4. It should be noted that the results for a single-stage system using any objective function led to the same optimal value of the decision variables. In this regard, the maximization of the first law efficiency provides enough power to balance the cost of the whole cycle thus the annual cost of electricity ($\tilde{C}$) is reduced to its minimal value. This is the reason why in Table 4 there is only one column for the

Table 1: Operating conditions of a single RC.

Parameter	Value	Units
nH	1	kmol s^{-}1
Twmx	90(363.15)	°C(K)
Twmn	70(342.15)	°C(K)
TWCmx	30(303.15)	°C(K)
TWCmn	20(293.15)	°C(K)
η_P	0.5	-
η_T	0.8	-
η_{MP}	0.9	-
η_{MT}	0.8	-

Table 2: Components for the mixtures of the model.

Number	Code	Name
1	R-22	Chlorodifluoromethane
2	R-134a	1,1,1,2-Tetrafluoroethane
3	R-152a	1,1-Difluoroethane
4	R-245ca	1,1,2,2,3-Pentafluoropropane
5	R-C318	Octafluorocyclobutane

Table 3: Parameters used for equations 55 through 64

Component	$cpx1_i$	$cpx2_i$	$cpx3_i$	$cpl1_i$	$cpl2_i$	$cpl3_i$
1	-9.96E-05	0.163	17.709	0.002	-0.648	155.312
2	-1.03E-04	0.243	22.179	0.002	-1.051	245.691
3	-5.29E-05	0.188	16.754	0.002	-0.964	218.717
4	-9.57E-05	0.304	34.026	0.002	-0.848	268.177
5	-3.29E-04	0.52	30.535	0.002	-0.447	213.338

	Single	Cascade η		Cascade $\tilde{C}$		Series η		Series $\tilde{C}$	
s	-	1	2	1	2	1	2	1	2
z_1	0.8435	0.0787	0.1032	0.1703	0.034	0	0	0	0
z_2	0	0	0.2891	0	0.75	0.6396	0.6885	0.6666	0.7331
z_3	0	0.6919	0	0.0971	0	0	0	0	0
z_4	0.0348	0.2294	0.1896	0.1306	0.2161	0.2295	0.224	0.2267	0.221
z_5	0.1217	0	0.418	0.6021	0	0.1309	0.0876	0.1068	0.0459
P_{High}	24.69	17.32	7.89	17.43	15.58	18.67	14.93	18.65	14.85
$\mathrm{TS}_{\mathrm{Sub,High}}$	303.37	319.87	298.94	315.23	300.77	301.23	300.95	301.42	301.30
$T_{\mathrm{Bubl,High}}$	339.67	341.65	314.01	344.16	336.43	347.03	336.61	346.59	335.91
$T_{\mathrm{Dew,High}}$	345.00	349.87	322.47	354.03	344.80	354.18	344.41	353.77	343.75
$\mathrm{TS}_{\mathrm{Over,High}}$	358.15	358.15	325.50	358.15	350.74	358.15	348.15	358.15	348.15
P_{Low}	9.96	9.93	5.09	16.45	5.92	5.49	5.62	5.58	5.76
$\mathrm{TS}_{\mathrm{Sub,Low}}$	301.12	318.46	298.60	315.18	299.48	299.64	299.78	299.82	300.14
$T_{\mathrm{Bubl,Low}}$	301.12	318.46	298.60	341.57	299.48	299.64	299.78	299.82	300.14
$T_{\mathrm{Dew,Low}}$	308.35	328.19	307.80	351.58	310.15	309.56	309.69	309.74	310.04
$\mathrm{TS}_{\mathrm{Over,Low}}$	317.21	334.93	314.68	355.74	318.29	317.65	317.06	317.91	317.51
n	0.1000	0.0898	0.0765	0.0832	0.0777	0.0374	0.0388	0.0376	0.0391
nC	2.3890	2.3668		2.3755		1.1695	1.1980	1.1701	1.1995
W_T	0.1600	0.1020	0.0793	0.0090	0.1777	0.2175	0.1767	0.2154	0.1725
W_P	0.0278	0.0120	0.0020	0.0020	0.0020	0.0020	0.0020	0.0020	0.0020
η	**0.0685**	**0.0771**		0.0737		**0.0768**		0.0760	
$\tilde{C}$	**1.0219**	1.3482		**1.3132**		1.0978		**1.0974**	
N_{var}	4750	9517		9592		9501		9600	
N_{eq}	5041	10105		10180		10095		10195	
CPU	24	177		190		63		86	
Tk_s	-	-		-		353.15		353.15	
$\hat{Y}_s^{\mathrm{liq}}$	-	False		False		-		-	
$\hat{Y}_s^{\mathrm{2P}}$	-	True		True		-		-	
$\check{Y}_s^{\mathrm{vap}}$	-	False		False		-		-	
$\check{Y}_s^{\mathrm{2P}}$	-	True		True		-		-	

Table 4: Results, P_{High} in bar, T and TS in K, $\tilde{C}$ in \$ MWh^{-1}, n in kmol s^{-1}, W in kJ/Hu, CPU in seconds

single-stage system. The optimal mixture only requires three of the available components with a large amount of the first component. The pressure and temperature processing conditions show that the cycle must be run at a pressure slightly larger than 24 bar, with the super heating profile ($\mathrm{TS}_{\mathrm{Over,High}} - T_{\mathrm{Dew,High}}$) of about 13 K. On the other hand, the multi-stage models always feature values below the high-pressure level of the single stage cycle. Moreover, the single-stage configuration features roughly the least expensive electricity in comparison to other multi-stage configurations, as shown by the value of the $\tilde{C}$ variable. In Figure 11 the stacked updated bare cost of equipment and overall water cost is displayed for all the processing configurations. The single stage configuration is clearly the least expensive since it requires the least number of modules (i.e. one turbine and pump, two heat exchangers).

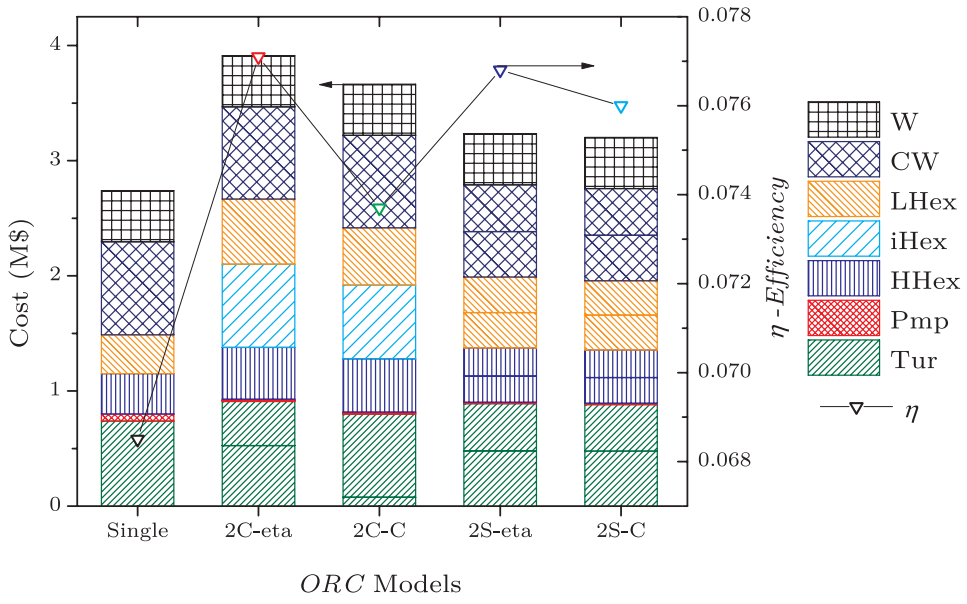

Figure 11: Cost distribution for their respective models and efficiencies. 2C-eta:Cascade with η, 2C-C:Cascade with $\tilde{C}$; 2S-eta:Series with η, 2S-C:Series with $\tilde{C}$. The cost displayed are Turbine, Pump; High-P (HHex), Low-P (LHex) and intermediate (iHex) heat exchangers; overall cooling water (CW) and water for heat source (W)

The multi-stage cascade configuration features cycles with larger efficiencies compared to similar values for the single-stage configuration. The maximization of the efficiency in

multi-stage cascade configurations leads to a value about 12 % higher than the corresponding one for the single-stage configuration. However, this consistently raises the equipment cost, mainly because of the need of an intermediate exchanger (iHex area on Fig. 11) that is not required in any other configuration.

In this configuration solving the optimization problem using the two objective functions led to different optimal solutions, because the higher cost of equipment is not balanced with the power production in the case of the maximization of the efficiency. So, using the second objective function leads to a less efficient but more economical design. However, both optimal values are above the annual cost of the single-stage configuration.

It was also found that the subsequent stages for the multi-stage cascade configuration require lower pressure, due to the temperature decrease as the stages are introduced. Moreover, it should be remarked that the stages feature different mixture composition between them. This is not the case for the multi-stage series configuration where each stage features the same components with similar composition.

The phase matching variables (Y_s's) show that both objective functions are optimal when two-phase regions are selected ($\hat{Y}_s^{2P}$ and $\check{Y}_s^{2P}$ are true). This suggest that the profiles are brought closer together without impacting the energy production when the stages are matched at two phase regions, and since the two profiles are closer, the intermediate heat exchanger is more expensive as shown in Figure 11. It is clear that the most significant issue in this kind of configuration is the intermediate phase change heat exchanger, which increases the overall cost by a significant amount.

In terms of the efficiency of the RC, the multi-stage series configuration shows results as efficient as those obtained using a multi-stage cascade configuration but with less cost. In this case both objective functions led to similar results. Hence, as the case of the single stage, both cost and energy production are almost in balance at the optimal point, meaning that similar results are obtained by using any of the proposed objective functions. The results display a decrease in pressure as additional stages are considered mainly

because the temperature of the heat source also decreases along the stages. However, the composition and the low pressure level of each stage show roughly the same values, which may suggest that it is possible to use almost similar mixtures and equipment in each stage with the exception of the pumps and vaporizers. Nevertheless, the overall cost of this configuration will always be larger than the cost of the single stage for the same reasons previously discussed regarding the cascade configuration. The main difference between these two configurations is that there is no intermediate heat exchanger in the series configuration. Overall, this will result in a less expensive cycle. It should be noted that with the inclusion of a new stage in the series configuration, the flows of cooling water and working fluid were almost halved, because each stage is absorbing a fraction of what the single-stage configuration does.

4.2 Impact at temperature of heat source

Another important issue is what happens when more than two stages are implemented in both multi-stage configurations over different temperatures of the heat source. Three temperatures (90, 100 and 110 °C) were tested with the cascade and series multi-stage configurations with two through five stages and using both objective functions. Additionally, an "hybrid" of the two configurations was tested with 2 × 2 cycles (Figure 12). This last process configuration can be generated through the merging of the inter-stage equations of the cascade and the heat source equations of the series model, and was chosen because of its problem size (roughly the same as a 4 stage cascade model). The results are displayed in Figures 13 and 14 for the cycle efficiency and annual cost, respectively. It should be pointed out that the cycle efficiency will increase when the temperature is raised no matter what configuration is used. Moreover, the cost per annual MWh ratio ($\tilde{C}$) will decrease because there is more power generated. The single-stage configuration was the most efficient (except for the 90 °C case which was commented on previously). It is also

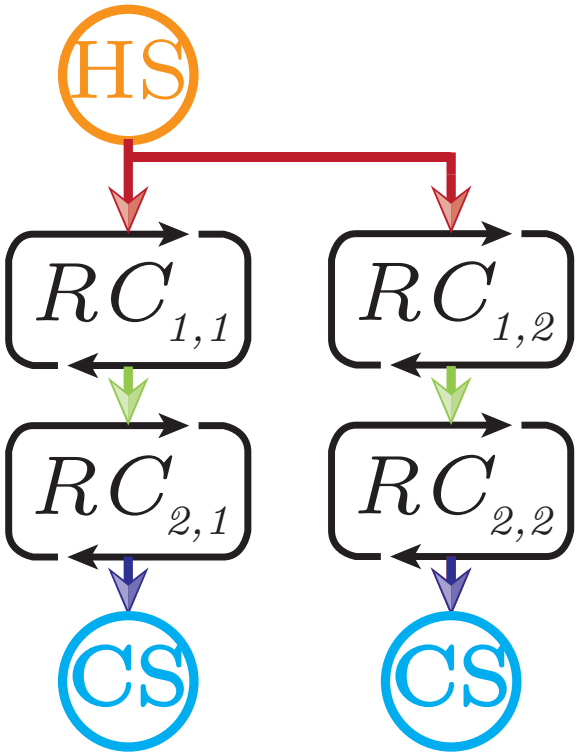

Figure 12: Cascade-Series 2 × 2 processing configuration

the least expensive model as showed in Figures 13 (a)-(c). In the case of the multi-stage cascade configuration the behavior can be generalized. The efficiency will decrease and the cost will rise steadily as new stages are added. One of the reasons for this behavior is that every new stage also requires a phase change inter-stage heat exchanger which is expensive and also will restraint the temperatures at which power is generated, because a minimal temperature difference is required as driving force for the heat exchange process to occur. In addition, the Y_s variables were found to be true, further generalizing the statements of the two stage-cascade phase match.

Although the multi-stage cascade configuration does not provide better results than the single-stage configuration, the cycle efficiencies of the two- and single- stages configurations are close as the temperature of the heat source varies. This is not the case for the cost per MWh ratio ($\tilde{C}$) where there is a consistent gap because of the inter-stage heat

exchanger as previously discussed. The results of the series multi-stage configuration are more regular since there is little variation as new stages are added in consistence with the two-stage configuration results. The absorbed heat in each stage is a proportional fraction of what the single-stage model does. Therefore, when a new stage is added the costs will be balanced and the cost ratio ($\tilde{C}$) will remain almost constant. In comparison with the single-stage, the multi-stage series configuration is less efficient no matter the number of stages, except for the 90 °C two-stage configuration case. This, in combination with the cascade results, suggest that the multi-stage configurations feature almost no improvement when the temperature is raised over the single-stage. Finally, the 2×2 hybrid configuration features almost the same level of thermodynamic efficiency (η) with respect to the tree-stage cascade model, but with lower electricity annual cost. However, the results are not better than the two-stage configuration or the single-stage process.

In summary, the multi-stage configurations were only effective at only one temperature. For the kind of organic fluids considered in this work, the single-stage model will be always the best choice. Although, the availability and size of equipment of the multi-stage configuration could possibly be an advantage over the single-stage process, especially when the series configuration is adopted, since the efficiency and cost are kept almost constant with stage inclusion. It also could be possible that in a dynamic environment, some configuration would be more well-behaved than the others in terms of process operability. In the case of the cascade configuration, the main difficulty is the inter-stage heat exchanger, which could be substituted by a direct contact heat transfer scheme, and thus overcoming the limitations of efficiency and cost. However, from a computational point of view, this will require a larger number of variables and equations since more regions of variable composition must be included.

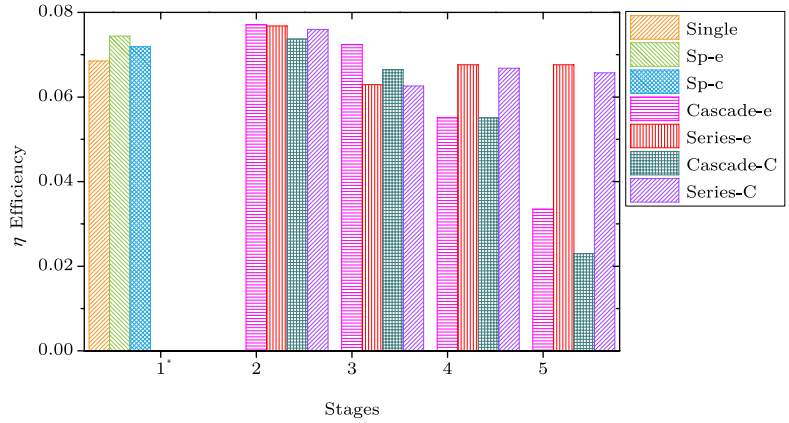

(a) η at 363.15 K (90 °C)

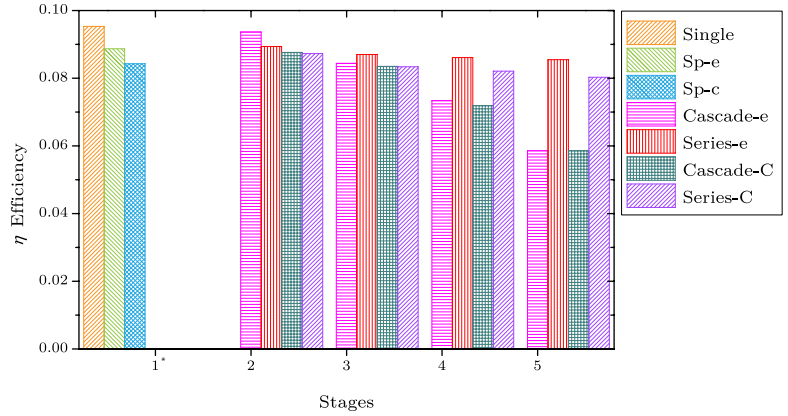

(b) η at 373.15 K (100 °C)

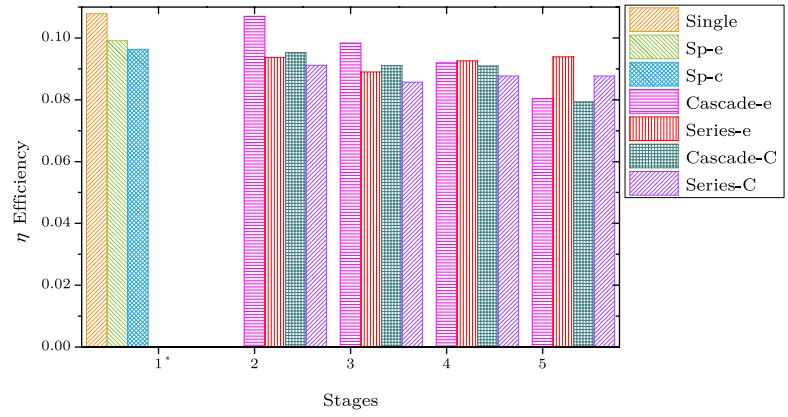

(c) η at 383.15 K (110 °C)

Figure 13: Efficiency η for the configurations at different temperatures. Single stage, Sp-e (Series-Cascade efficiency), Sp-c (Series-Cascade $\tilde{C}$), Cascade-e (efficiency), Series-e (efficiency), Cascade-C ($\tilde{C}$), Series-C ($\tilde{C}$)

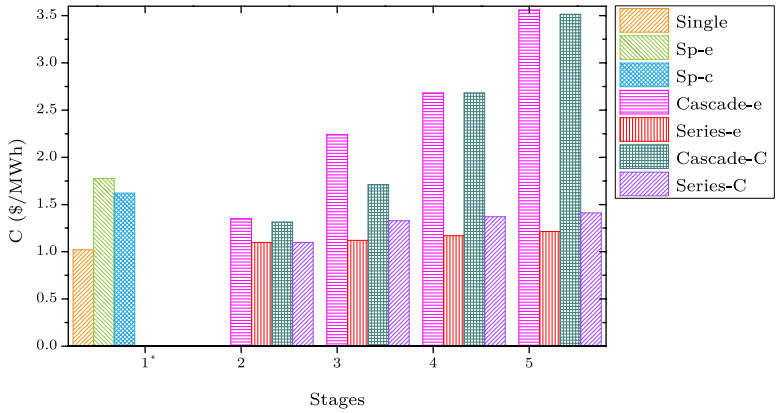

(a) $\tilde{C}$ at 363.15 K (90 °C)

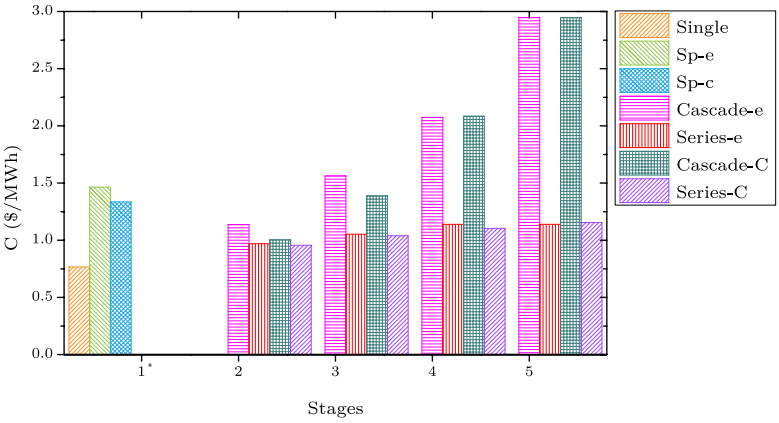

(b) $\tilde{C}$ at 373.15 K (100 °C)

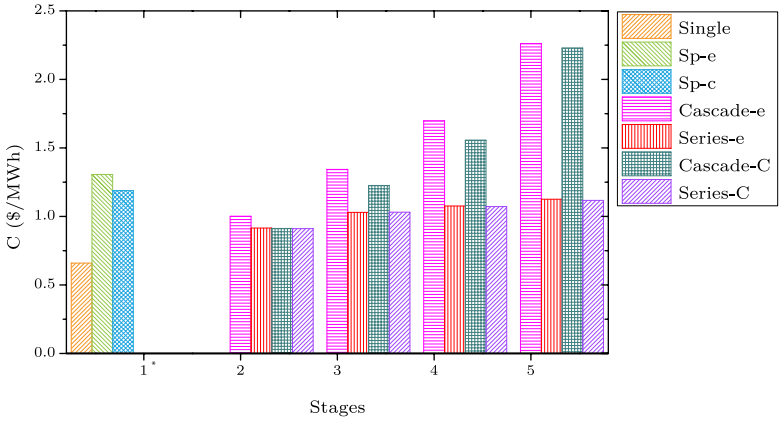

(c) $\tilde{C}$ at 383.15 K (110 °C)

Figure 14: Annual Cost for the configurations at different temperatures.

5 Conclusions

The heat available at low temperature is a potential source for power through the Rankine cycle. But because of the difficulties implied by low temperature, the Rankine cycle must be modified. The modifications currently proposed by various authors have dealt with the working fluid selection, and the Rankine cycle optimization. In this work we deploy two multiple coupled cycles: the series and cascade configurations. If all the cycle variables are selected in a systematic way, an improvement of performance is expected. Additionally, if we consider the working fluid of a mixture of defined components as a degree of freedom, it is possible that the simultaneous determination of these variables generates an even better improvement. All the considerations involving the multi-stage Rankine cycle design with mixtures as working fluids, were implemented into an algebraic model that was solved for optimality with deterministic approaches. For this, two objective functions were analyzed individually. The implementation of the cascade model was found to require complex constraints that can be formulated through generalized disjunctive programming (GDP). The results show that the multistage approaches are only useful for the two-stage case at low temperature in terms of the efficiency. But, they are intrinsically more expensive than the single stage Rankine cycle because of the necessity of more equipment for every single situation. As temperature progresses, none of the multistage configurations is better than the single stage. For the cascade cycle, the phase matching logical variables show that in the case of cascade configurations, the best match is always at the two phase region. But the existence of this intermediate heat transfer stage results in the more costly configuration because this requires an expensive heat exchanger, and as stages are added the cost raises steadily. The series configuration, although marginally less efficient than the single stage, turned out to keep almost the same objectives as stages are added. Although the results favored the single stage approach as the temperature increases, it can be worth to verify if multistage Rankine cycles display better operability, controllability

features and to examine how uncertainty affects the results presented in this work. Both topics will be addressed in future work.

Nomenclature

Indexes

$i, j \in I$	component of the mixture
$s \in S_{TG}$	stage
S_L	last stage
$k, m, n \in M$	functional group
$f \in F$	phase
L	liquid
V	vapor
$\pi \in \Pi$	equilibrium point
$p \in L$	pressure level
$\underline{o} \in \underline{O}$	subcool point
$\overline{o} \in \overline{O}$	superheat point
O	nonequilibrium points

Condensed notation of constraints and variables

$\overline{\boldsymbol{Z}}_s$	EOS equations
$\overline{\boldsymbol{G}}_s$	activity coefficients equations
$\overline{\boldsymbol{B}}_s$	equilibrium and property equations
$\overline{\boldsymbol{\varphi}}_s$	operation constraints
$\overline{\boldsymbol{C}}_s$	cost equations
$\overline{\boldsymbol{U}}_s^1$	single stage constraints
$\overline{\boldsymbol{U}}_s^C$	multi-stage cascade constraints
$\overline{\boldsymbol{U}}_s^S$	multi-stage series constraints
$\bar{t}_s^L$ (liq)	multi-stage cascade LP liquid match
$\bar{t}_s^L$ (2P)	multi-stage cascade LP 2-phase match
$\bar{t}_s^U$ (vap)	multi-stage cascade HP liquid match
$\bar{t}_s^U$ (2P)	multi-stage cascade HP 2-phase match
$\overline{\boldsymbol{P}}_s$	Pressure
$\overline{\boldsymbol{T}}_s$	Temperatures
$\overline{\boldsymbol{z}}_s$	Compositions
$\overline{\boldsymbol{X}}$	Operating variables(e.g. molar flows, HX areas, fugacity coefficients, etc)

Variables

Symbol	Description	Units
$(A_{e'}^i)_s$	Heat exchanger intermediate two-phase	m^2
$(A_{l'}^i)_s$	Heat exchanger intermediate liquid	m^2
$(A_{v'}^i)_s$	Heat exchanger intermediate vapor	m^2
$\left(A_{e'}^L\right)_s$	Heat exchanger area two-phase LP	m^2
$\left(A_{l'}^L\right)_s$	Heat exchanger area liquid LP	m^2
$\left(A_{v'}^L\right)_s$	Heat exchanger area vapor LP	m^2
$A_{e'}^H$	Heat exchanger area two-phase HP	m^2

$A^H_{l'}$	Heat exchanger area liquid HP	m^2
$A^H_{v'}$	Heat exchanger area vapor HP	m^2
$\hat{a}S_{s\bar{o}p}$	Mixture EOS var n-eq.	dimensionless
$\hat{a}S'_{s\bar{o}p}$	Mix. EOS variable temp. derivative n-eq.	bar cm^3 $kmol^{-1}$ K^{-1}
aR_{isp}	EOS variable Ref.	dimensionless
aR'_{isp}	EOS variable temp. derivative ref.	K^{-1}
$aS'_{is\bar{o}p}$	EOS variable temp. derivative n-eq.	K^{-1}
au_{is}	EOS variable	dimensionless
aup_{is}	EOS variable pure	K^{-1}
a'_{isp}	EOS variable temp. derivative	K^{-1}
$a\hat{u}_s$	EOS variable	dimensionless
$\hat{a}'_{sp}$	Mix. EOS variable temp. derivative	bar cm^3 $kmol^{-1}$ K^{-1}
$a\hat{u}p_s$	Mixture EOS variable	bar cm^3 $kmol^{-1}$ K^{-1}
$(B_{CP})_s$	Updated bare pump cost	\$
$(B_{CT})_s$	Updated bare turbine cost	\$
$(B^i_{CX})_s$	Updated bare heat exchanger cost intermediate	\$
B^H_{CX}	Update bare heat exchanger cost HP	\$
$\left(B^L_{CX}\right)_s$	Update bare heat exchanger cost HP	\$
$\hat{b}_{s\pi p}$	Mixture EOS variable	cm^3 $kmol^{-1}$
bR_{isp}	EOS variable Ref.	dimensionless
$\hat{bS}_{s\bar{o}p}$	Mix. EOS variable n-eq.	dimensionless
bu_s	EOS variable	dimensionless
CWW_{yr}	Cost of cooling water	\$
$\tilde{C}$	Cost per annual MWh	\$ MWh^{-1}
$\left(DHR^{id}\right)_{isp}$	Ideal gas enthalpy change ref.	kJ/Hu
$\left(DhR^{lv}\right)_{isp}$	Vaporization enthalpy change	kJ/Hu

$(\mathrm{fR}_T)_{isp}$	EOS temp. Funct. at ref. temp.	dimensionless
E_G	Electricity generated 1 yr basis	MWh
$(\mathrm{fR}'_T)_{isp}$	EOS variable temp. Derivative ref.	K^{-1}
$(\mathrm{fS}_T)_{is\bar{o}p}$	EOS temp. Funct. at nonequilibrium temp.	dimensionless
$(f_T)_{is\pi p}$	EOS temperature function	dimensionless
$(f'_T)_{isp}$	EOS variable temp. Derivative	K^{-1}
$(\mathrm{fS}'_T)_{is\bar{o}p}$	EOS variable temp. Derivative n-eq.	K^{-1}
$K_{is\pi p}$	Equilibrium ratio	dimensionless
$\left(\mathrm{LMTD}^H_{e'}\right)_s$	Log mean temperature difference HP 2-phase	K
$\left(\mathrm{LMTD}^H_{l'}\right)_s$	Log mean temperature difference HP liquid	K
$\left(\mathrm{LMTD}^H_{v'}\right)_s$	Log mean temperature difference HP vapor	K
$\left(\mathrm{LMTD}^i_{e'}\right)_s$	Log mean temperature difference inter. H-ex. 2-phase	K
$\left(\mathrm{LMTD}^i_{l'}\right)_s$	Log mean temperature difference inter. H-ex. liquid	K
$\left(\mathrm{LMTD}^i_{v'}\right)_s$	Log mean temperature difference inter. H-ex. vapor	K
$\left(\mathrm{LMTD}^L_{e'}\right)_s$	Log mean temperature difference LP 2-phase	K
$\left(\mathrm{LMTD}^L_{l'}\right)_s$	Log mean temperature difference LP liquid	K
$\left(\mathrm{LMTD}^L_{v'}\right)_s$	Log mean temperature difference LP vapor	K
$\mathrm{dHHS}_{s\pi}$	Enthalpy point of heat source	kJ/Hu
DHiu_{is}	Ideal enthalpy change	kJ/Hu
fTu_{is}	EOS temperature function	dimensionless
fTup_{is}	EOS T function pure T. der	K^{-1}
F_C	Overall Updated cost of equipment	$
$\mathrm{GS}'_{s\bar{o}p}$	Gibbs excess temp. der.	bar cm^3 kmol^{-1} K^{-1}
$\mathrm{GS}_{s\bar{o}p}$	Gibbs excess dimensionless n-eq.	dimensionless
G'_{sp}	Gibbs excess temp. der.	bar cm^3 kmol^{-1} K^{-1}
$G_{s\pi Vp}$	Gibbs excess dimensionless	dimensionless

$\mathrm{Hp}_{s\pi p}$	Enthalpy point at eq.	kJ/Hu
$\left(H^R\right)_{sp}$	Residual enthalpy	dimensionless
HRRF_{isp}	Ref. residual enthalpy	dimensionless
HRu_s	Residual enthalpy	dimensionless
$(\mathrm{HR})_{s\bar{o}p}$	Residual enthalpy n-eq.	dimensionless
$\mathrm{HS}_{s\bar{o}p}$	Vapor enthalpy n-eq.	kJ/Hu
$\mathrm{hS}_{s\underline{o}p}$	Liquid enthalpy n-eq.	kJ/Hu
h_{sp}	Liquid enthalpy	kJ/Hu
H_{sp}	Vapor enthalpy	kJ/Hu
Hup_{sp}	Vapor enthalpy	kJ/Hu
$\mathrm{lGP}_{iks\pi p}$	Activity contribution mix. Pure	dimensionless
n_s	Mole flow of working fluid	kmol s^{-1}
nC_s	Mole flow of heat sink	kmol s^{-1}
$P^{\mathrm{sat}}_{is\pi p}$	Saturation Pressure	bar
P_{sp}	Pressure at level s	bar
PWW_{yr}	Cost of water (Heat source)	\$ m-3
Q_{sp}	Heat	kJ/Hu
$\left(\mathrm{sTR}^{id}\right)_{isp}$	Ideal gas entropy change ref.	kJ K^{-1} /Su
$(\mathrm{SR})_{s\bar{o}p}$	Residual entropy n-eq.	dimensionless
$\left(S^R\right)_{sp}$	Residual entropy	dimensionless
$\left(S^R\right)_{sp}$	Ref. residual entropy	dimensionless
$\mathrm{SS}_{s\bar{o}p}$	Liquid entropy	kJ K^{-1} /Su
$\mathrm{sS}_{s\underline{o}p}$	Liquid entropy n-eq.	kJ K^{-1} /Su
s_{sp}	Liquid entropy	kJ K^{-1} /Su
S_{sp}	Liquid entropy	kJ K^{-1} /Su
$(S_P)_s$	Pump design value	gpm $\times$ psi

$(S_T)_s$	Turbine design value	hp
Tk_s	Intermediate temperature of stage	K
tL_s	Low pressure match	K
TRF_{isp}	Reference temperature	K
TS_{sop}	Temperature at nonequilibrium	K
tU_s	High pressure match	K
$\mathrm{TwC}_{s\pi}$	Heat sink temperature at equilibrium	K
$\mathrm{TwH}_{s\pi}$	Heat source temperature at equilibrium	K
VL_s	Vapor fraction low pressure	K
V_C	overall cost of utilities	$
$T_{s\pi p}$	Temperature at equilibrium	K
$x_{isf\pi p}$	equilibrium composition	dimensionless
$X_{ms\pi fp}$	functional group mole fraction	dimensionless
$\hat{Y}_s^{\mathrm{liq}}$	Boolean variable HP liquid match	{true,false}
$\hat{Y}_s^{\mathrm{2P}}$	Boolean variable HP two phase match	{true,false}
$\check{Y}_s^{\mathrm{vap}}$	Boolean variable LP vapor match	{true,false}
$\check{Y}_s^{\mathrm{2P}}$	Boolean variable LP two phase match	{true,false}
$(W_P)_s$	Work (positive) pump	kJ/Hu
$(W_T)_s$	Work (positive) turbine	kJ/Hu
$Z_{is\pi p}^{\mathrm{sat}}$	Saturation Comp. Fact.	dimensionless
ZR_{isp}	Ref. Compressibility Factor	dimensionless
Zu_s	Compressibility factor	dimensionless
$\hat{Z}_{s\pi p}$	Mix. Compressibility factor	dimensionless
$\hat{\mathrm{Z}}\mathrm{S}_{s\bar{o}p}$	Mix. Compressibility factor n-eq.	dimensionless
z_{is}	Global composition	dimensionless
η_I	Efficiency by the 1st law of Thermodynamics	dimensionless

$\alpha_{is\pi p}$	Mixture EOS variable	dimensionless
$\hat{\alpha}_{s\pi p}$	Mixture EOS variable	dimensionless
$\overline{\alpha}_{is\pi p}$	Molar part. EOS variable	dimensionless
$\hat{\alpha}_{s\pi p}$	Mixture EOS variable	dimensionless
$\hat{\beta}_{s\pi p}$	Mixture EOS variable	dimensionless
$\beta^{\text{sat}}_{is\pi p}$	EOS var at saturation	dimensionless
$\left(\Delta H^{id}\right)_{isp}$	Ideal gas enthalpy change	kJ/Hu
$(\Delta \text{Hs})_{is\bar{o}p}$	Ideal gas enthalpy change n-eq.	kJ/Hu
ΔHl_{isp}	Liquid enthalpy change	kJ/Hu
$\Delta \text{HlS}_{is\underline{o}p}$	Liquid enthalpy change n-eq.	kJ/Hu
ΔHe_s	Enthalpy change at stage	kJ/Hu
$\left(\Delta S^{id}\right)_{isp}$	Ideal gas entropy change	kJ K^{-1} /Su
$(\Delta \text{Ss})_{is\bar{o}p}$	Ideal gas entropy change n-eq.	kJ K^{-1} /Su
ΔSl_{isp}	Liquid entropy change	kJ K^{-1} /Su
$\Delta \text{SlS}_{is\underline{o}p}$	Liquid entropy change n-eq.	kJ K^{-1} /Su
$\Psi_{mks\pi p}$	UNIFAC interaction var.	dimensionless
ψ_u	Vapor fraction high pressure	dimensionless
$\theta_{ms\pi fp}$	functional group area fraction	dimensionless
$\ln \gamma_{is\pi fp}$	Activity coefficient natural logarithm	dimensionless
$\ln \gamma^C_{is\pi fp}$	Activity coefficient combinatorial	dimensionless
$\ln \gamma^R_{is\pi fp}$	Activity coefficient residual	dimensionless
$\ln \Gamma_{ks\pi fp}$	Activity contribution mix.	dimensionless
$(\ln \Phi^{\text{sat}})_{is\pi p}$	Saturation fugacity coefficient	dimensionless
$\left(\ln \hat{\Phi}\right)_{is\pi p}$	Mixture fugacity coefficient	dimensionless

Parameters

Symbol	Description	Units
A1	PSRK parameter (-0.64666)	dimensionless
a_{mn}	UNIFAC binary interaction parameter	K
b_i	EOS parameter ($0.008446 R_g \mathrm{Tc}_i/\mathrm{Pc}_i$)	$\mathrm{cm}^3\ \mathrm{kmol}^{-1}$
$c_{\omega,i}$	Acentric function ($0.48 + 1.574\omega_i - 0.176\omega_i^2$)	dimensionless
C_{0T}	Cost factor turbine	$
C_{0X}	Heat exchanger cost coefficient	$
C_{0P}	Cost coefficient pump	$
$C_{1,i} - C_{7,i}$	Vapor pressure parameters	see Eq. 39 & 40
$\mathrm{cpx1}_i$	Ideal gas heat capacity parameter	$\mathrm{kJ\ K}^{-3}$
$\mathrm{cpx2}_i$	Ideal gas heat capacity parameter	$\mathrm{kJ\ K}^{-2}$
$\mathrm{cpx3}_i$	Ideal gas heat capacity parameter	$\mathrm{kJ\ K}^{-1}$
$\mathrm{cpl1}_i$	Liquid heat capacity parameter	$\mathrm{kJ\ K}^{-3}$
$\mathrm{cpl2}_i$	Liquid heat capacity parameter	$\mathrm{kJ\ K}^{-2}$
$\mathrm{cpl3}_i$	Liquid heat capacity parameter	$\mathrm{kJ\ K}^{-1}$
CEPCI	CE plant cost index (579.8)	dimensionless
CSF_0	Cost of water adjustment parameter	$ m^{-}3
CSF_{yr}	Cost of water adjustment parameter for year yr	$ m^{-}3
DHF_i	Formation enthalpy change	$\mathrm{kJ\ kmol}^{-1}$
DGF_i	Formation Gibbs energy change	$\mathrm{kJ\ kmol}^{-1}\ \mathrm{K}^{-1}$
DHHT	Heat source overall enthalpy change ($\int_{Twmn}^{Twmx} Cp_H dT$)	kJ /Hu
F_{0P}	Update factor pump	$
F_{0T}	Update factor turbine	$
F_{0X}	Update factor HX	$
Hu	Enthalpy scaling factor (10^4)	dimensionless
l_j	UNIFAC parameters	dimensionless

nH	Heat source mole flow	kmol s^{-1}
Pc_i	Critical pressure	bar
Q_k	UNIFAC parameters	dimensionless
q_i	UNIFAC parameters	dimensionless
R_g	Gas constant	bar cm^3 $kmol^{-1}$ K^{-1}
R_k	UNIFAC parameters	dimensionless
r_i	UNIFAC parameters	dimensionless
Su	Entropy factor (10^3)	dimensionless
S_{0T}	Cost factor turbine	hp
S_{0X}	Heat exchanger cost coefficient	m^2
S_{0P}	Cos coefficient pump	gpm $\times$ psi
Twmn	Heat source minimum temperature	K
Twmx	Heat source maximum temperature	K
TwCmn	Heat sink minimum temperature	K
TwCmx	Heat sink maximum temperature	K
Tc_i	Critical temperature	K
Tbr_i	Normal boiling temperature	K
TP_{im}	UNIFAC pure molecule fraction area	dimensionless
$U_{l'}$	Overall heat transfer coef. liquid	kW K^{-1} m^{-1}
$U_{e'}$	Overall heat transfer coef. two phase	kW K^{-1} m^{-1}
$U_{v'}$	Overall heat transfer coef. vapor	kW K^{-1} m^{-1}
$U^i_{l'}$	Overall heat transfer coef. intermediate liquid	kW K^{-1} m^{-1}
$U^i_{e'}$	Overall heat transfer coef. intermediate two phase	kW K^{-1} m^{-1}
$U^i_{v'}$	Overall heat transfer coef. intermediate vapor	kW K^{-1} m^{-1}
yr	year	1,2,...,yrL
XP_{im}	UNIFAC mole fraction pure mole.	dimensionless

α_P	Cost coefficient pump	dimensionless
α_T	Cost factor turbine	dimensionless
α_X	Heat exchanger cost coefficient	dimensionless
$\Delta \mathrm{hB}_i^{\mathrm{LV}}$	Normal boiling point enthalpy change	kJ kmol^{-1}
ν_{im}	UNIFAC group frequency on mole. i	dimensionless
η_{MP}	Mechanical efficiency pump	dimensionless
η_{MT}	Mechanical efficiency turbine	dimensionless
η_T	Turbine efficiency	dimensionless
η_P	Pump efficiency	dimensionless
ψ_π	Vapor fraction	dimensionless

References

[1] Badr, O.; Probert, S.; O'Callaghan, P. Selecting a working fluid for a Rankine-cycle engine. *Appl. Energ.* 21(1):1–42, **1985**.

[2] Larjola, J. Electricity from industrial waste heat using high-speed organic Rankine cycle (ORC). *Int. J. Prod. Econ.* 41(1):227–235, **1995**.

[3] Linke, P.; Papadopoulos, A. I.; Seferlis, P. Systematic Methods for Working Fluid Selection and the Design, Integration and Control of Organic Rankine Cycles-A Review. *Energies* 8(6):4755–4801, **2015**.

[4] Mavrou, P.; Papadopoulos, A. I.; Seferlis, P.; Linke, P.; Voutetakis, S. Selection of working fluid mixtures for flexible Organic Rankine Cycles under operating variability through a systematic nonlinear sensitivity analysis approach. *Appl. Therm. Eng.* **2015**.

[5] Braimakis, K.; Preißinger, M.; Brüggemann, D.; Karellas, S.; Panopoulos, K. Low grade waste heat recovery with subcritical and supercritical Organic Rankine Cycle based on natural refrigerants and their binary mixtures. *Energy* **2015**.

[6] Lampe, M.; Stavrou, M.; Bucker, H.; Gross, J.; Bardow, A. Simultaneous optimization of working fluid and process for organic Rankine cycles using PC-SAFT. *Ind. Eng. Chem. Res.* 53(21):8821–8830, **2014**.

[7] Lecompte, S.; Huisseune, H.; van den Broek, M.; Vanslambrouck, B.; De Paepe, M. Review of organic Rankine cycle (ORC) architectures for waste heat recovery. *Renew. Sust. Energ. Rev.* 47:448–461, **2015**.

[8] Molina-Thierry, D. P.; Flores-Tlacuahuac, A. Simultaneous optimal design of organic mixtures and Rankine cycles for low-temperature energy recovery. *Ind. Eng. Chem. Res.* 54(13):3367–3383, **2015**.

[9] Kosmadakis, G.; Manolakos, D.; Kyritsis, S.; Papadakis, G. Economic assessment of a two-stage solar organic Rankine cycle for reverse osmosis desalination. *Renew. Energ.* 34(6):1579–1586, **2009**.

[10] Morisaki, T.; Ikegami, Y. Maximum power of a multistage Rankine cycle in low-grade thermal energy conversion. *Appl. Therm. Eng.* 69(1):78–85, **2014**.

[11] Yun, E.; Kim, D.; Yoon, S. Y.; Kim, K. C. Experimental investigation of an organic Rankine cycle with multiple expanders used in parallel. *Appl. Energ.* 145:246–254, **2015**.

[12] Li, T.; Zhang, Z.; Lu, J.; Yang, J.; Hu, Y. Two-stage evaporation strategy to improve system performance for organic Rankine cycle. *Appl. Energ.* 150:323–334, **2015**.

[13] Stijepovic, M. Z.; Papadopoulos, A. I.; Linke, P.; Grujic, A. S.; Seferlis, P. An exergy composite curves approach for the design of optimum multi-pressure organic Rankine cycle processes. *Energy* 69:285–298, **2014**.

[14] Smith, J.; Van Ness, H.; Abbott, M. Chemical engineering thermodynamics. *McGraw-Hill, NY* **2001**.

[15] Holderbaum, T.; Gmehling, J. PSRK: A group contribution equation of state based on UNIFAC. *Fluid Phase Equilib.* 70(2):251–265, **1991**.

[16] Kamath, R. S.; Biegler, L. T.; Grossmann, I. E. An equation-oriented approach for handling thermodynamics based on cubic equation of state in process optimization. *Comput. Chem. Eng.* 34(12):2085–2096, **2010**.

[17] Fredenslund, A. *Vapor-liquid equilibria using UNIFAC: a group-contribution method.* Elsevier, **2012**.

[18] Kleiber, M. An extension to the UNIFAC group assignment for prediction of vapor-liquid equilibria of mixtures containing refrigerants. *"Fluid Phase Equilib.* 107(2):161–188, **1995**.

[19] Dahl, S.; Michelsen, M. L. High-pressure vapor-liquid equilibrium with a UNIFAC-based equation of state. *AIChE J.* 36(12):1829–1836, **1990**.

[20] Poling, B. E.; Prausnitz, J. M.; John Paul, O.; Reid, R. C. *The properties of gases and liquids*, volume 5. McGraw-Hill New York, **2001**.

[21] Henley, E. J.; Seader, J. *Equilibrium-Stage Separation Operations in Chemical Engineering*. John Wiley, **1981**.

[22] Rowley, R.; Wilding, W.; Oscarson, J.; Yang, Y.; Zundel, N.; Daubert, T.; Danner, R. DIPPR Data Compilation of Pure Chemical Properties. *Des. Inst. Phys. Prop.* **2006**.

[23] Aspen Technology Inc. Aspen Plus v8.4 **2014**. URL `https://www.aspentech.com/products/engineering/aspen-plus/`.

[24] Grossmann, I. E. Review of nonlinear mixed-integer and disjunctive programming techniques. *Optimization and Engineering* 3(3):227–252, **2002**.

[25] Trespalacios, F.; Grossmann, I. E. Review of Mixed-Integer Nonlinear and Generalized Disjunctive Programming Methods. *Chem. Ing. Tech.* 86(7):991–1012, **2014**.

[26] Kreith, F. *The CRC handbook of thermal engineering*. Springer Science & Business Media, **2000**.

[27] Awad, M. M. *Fouling of heat transfer surfaces*. INTECH Open Access Publisher, **2011**.

[28] Biegler, L. T.; Grossmann, I. E.; Westerberg, A. W. *Systematic methods for chemical process design*. Prentice Hall, Old Tappan, NJ (United States), **1997**.

[29] Access Intelligence. Plant Cost Index. *Chemical engineering [Online]* **2015**. URL `http://www.chemengonline.com/pci-home`.

[30] Ulrich, G. D.; Vasudevan, P. T. How to estimate utility costs. *Chemical Engineering* 113(4):66–69, **2006**.

[31] Brooke, A.; Kendrick, D.; Meeraus, A.; Raman, R. *GAMS: A User's Guide*. GAMS Development Corporation: Washington, DC, **1981**.

[32] Drud, A. S. CONOPT- a large-scale GRG code. *ORSA J. Comput.* 6(2):207–216, **1994**.

[33] Vecchietti, A.; Grossmann, I. E. LOGMIP: a disjunctive 0–1 non-linear optimizer for process system models. *Computers & Chemical Engineering* 23(4):555–565, **1999**.